Canada

FLUTTER ANALYSIS OF A TWO-DIMENSIONAL AIRFOIL WITH CUBIC NON-LINEAR RESTORING FORCE

by

B.H.K. Lee, P. LeBlanc

National Aeronautical Establishment

AERONAUTICAL NOTE

NAE-AN-36

NRC NO. 25438

86-03947/

NATIONAL AERONAUTICAL ESTABLISHMENT

SCIENTIFIC AND TECHNICAL PUBLICATIONS

AERONAUTICAL REPORTS:

Aeronautical Reports (LR): Scientific and technical information pertaining to aeronautics considered important, complete, and a lasting contribution to existing knowledge.

Mechanical Engineering Reports (MS): Scientific and technical information pertaining to investigations outside aeronautics considered important, complete, and a lasting contribution to existing knowledge.

AERONAUTICAL NOTES (AN): Information less broad in scope but nevertheless of importance as a contribution to existing knowledge.

LABORATORY TECHNICAL REPORTS (LTR): Information receiving limited distribution because of preliminary data, security classification, proprietary, or other reasons.

Details on the availability of these publications may be obtained from:

Publications Section,
National Research Council Canada,
National Aeronautical Establishment,
Bldg. M-16, Room 204,
Montreal Road,
Ottawa, Ontario
K1A 0R6

ÉTABLISSEMENT AÉRONAUTIQUE NATIONAL

PUBLICATIONS SCIENTIFIQUES ET TECHNIQUES

RAPPORTS D'AÉRONAUTIQUE

Rapports d'aéronautique (LR): Informations scientifiques et techniques touchant l'aéronautique jugées importantes, complètes et durables en termes de contribution aux connaissances actuelles.

Rapports de génie mécanique (MS): Informations scientifiques et techniques sur la recherche externe à l'aéronautique jugées importantes, complètes et durables en termes de contribution aux connaissances actuelles.

CAHIERS D'AÉRONAUTIQUE (AN): Informations de moindre portée mais importantes en termes d'accroissement des connaissances.

RAPPORTS TECHNIQUES DE LABORATOIRE (LTR): Informations peu disséminées pour des raisons d'usage secret, de droit de propriété ou autres ou parce qu'elles constituent des données préliminaires.

Les publications ci-dessus peuvent être obtenues à l'adresse suivante:

Section des publications
Conseil national de recherches Canada
Établissement aéronautique national
Im. M-16, pièce 204
Chemin de Montréal
Ottawa (Ontario)
K1A 0R6

UNLIMITED
UNCLASSIFIED

FLUTTER ANALYSIS OF A TWO-DIMENSIONAL AIRFOIL WITH CUBIC NON-LINEAR RESTORING FORCE

ANALYSE DE FLOTTEMENT D'UN PROFIL BIDIMENSIONNEL À L'AIDE D'UNE FORCE STABILISATRICE CUBIQUE NON-LINÉAIRE

by/par

B.H.K. Lee, P. LeBlanc*

National Aeronautical Establishment
* Co-op Student, University of Waterloo

AERONAUTICAL NOTE
NAE-AN-36
NRC NO. 25438

OTTAWA
FEBRUARY 1986

L.H. Ohman, Head/Chef
High Speed Aerodynamics Laboratory/
Laboratoire d'aérodynamique à hautes vitesses

G.M. Lindberg
Director/Directeur

SUMMARY

Flutter analysis of a two-dimensional airfoil with a cubic non-linear restoring force in the pitch degree of freedom is investigated. The structural dynamic equations of motion are integrated by a time marching finite difference scheme. Flutter is determined from conditions which give rise to either a divergent or limit-amplitude solution. Case studies using various airfoil parameters and coefficients of the non-linear term in the restoring force are carried out. The effect of initial conditions is studied by varying the displacement from equilibrium of the pitch angle at the start of the airfoil motion. For a soft spring, an increase in the initial angular displacement can induce flutter to occur below the linear flutter speed. Factors that have stabilizing and destabilizing effects are investigated. For a hard spring, divergent flutter is not encountered. Instead, the oscillations maintain a self-limited amplitude which is independent of initial angular displacement. The effects of airfoil parameters on the amplitudes of heave and pitch motions are studied.

RÉSUMÉ

L'étude consiste en une analyse de flottement dans le plan de tangage d'un profil bidimensionnel à l'aide d'une force stabilisatrice cubique non-linéaire. Les équations de mouvement dynamiques structurales sont intégrées par une méthode d'avancement du temps aux différences finies. Le flottement est déterminé à partir d'états qui donnent lieu à un résultat divergent ou à amplitude limitée. Des études de cas portent sur divers paramètres de profil et divers coefficients de terme non-linéaire dans la force stabilisatrice. On étudie l'effet sur les conditions initiales en faisant varier l'écart angulaire à partir de la position d'équilibre de l'angle de tangage au début du mouvement du profil. Lorsqu'on utilise un ressort faible, un accroissement de l'écart angulaire initial peut produire de flottements à une vitesse inférieure à la vitesse linéaire de ces vibrations. On étudie les facteurs ayant des effets de stabilisation et de déstabilisation. Lorsqu'on utilise un ressort plus fort, il ne se produit pas de flottements divergents. A la place des oscillations maintiennent une amplitude autolimitée, indépendante de l'écart angulaire initial. On étudie les effets des paramètres de profil sur l'amplitude des mouvements de pilonnement et de tangage.

CONTENTS

		Page
	SUMMARY	(iii)
	APPENDICES	(v)
	SYMBOLS	(v)
1.0	INTRODUCTION	1
2.0	ANALYSIS	3
	2.1 Two-Degree-of-Freedom Motion of a 2-D Airfoil	3
	2.2 Finite Difference Scheme	5
	2.3 Recurrence Formula for Aerodynamic Lift	6
	2.4 Starting Procedure	7
3.0	RESULTS AND DISCUSSIONS	8
	3.1 Flutter Boundaries for Soft Spring	8
	3.2 Limit-Cycle Flutter for Hard Spring	10
4.0	CONCLUSIONS	12
5.0	REFERENCES	13

ILLUSTRATIONS

Figure		Page
1	Two-Degree-of-Freedom Airfoil Motion	15
2	Effect of β on Non-Linear Restoring Force	16
3(a)	Time Variation of α in Stable Region for $\mu = 100$, $x_\alpha = 0.25$, $\bar{\omega} = 0.2$, $\beta = -3.0$, $\alpha_o = 10^\circ$ and $U_N^*/U_L^* = 0.96$	17
3(b)	Time Variation of α in Flutter Region for $\mu = 100$, $x_\alpha = 0.25$, $\bar{\omega} = 0.2$, $\beta = -3.0$, $\alpha_o = 10^\circ$ and $U_N^*/U_L^* = 0.973$	17
4	Effect of μ on the Flutter Boundaries for $\bar{\omega} = 0.2$, $x_\alpha = 0.25$	18
5	Flutter Boundaries for $\bar{\omega} = 0.2$, $\mu = 250$ and $x_\alpha = 0.1$	19
6	Flutter Boundaries for $\bar{\omega} = 0.2$, $\mu = 250$ and $x_\alpha = 0.4$	20
7	Flutter Boundaries for $\mu = 100$, $x_\alpha = 0.25$, $\bar{\omega} = 0.8$ and 1.2	21

ILLUSTRATIONS (Cont'd)

Figure		Page
8(a)	Time Variation of α in Stable Region for $\mu = 100$, $x_\alpha = 0.25$, $\bar{\omega} = 0.2$, $\beta = 0.3$, $\alpha_o = 10°$ and $U_N^*/U_L^* = 0.99$	22
8(b)	Time Variation of α in Flutter Region for $\mu = 100$, $x_\alpha = 0.25$, $\bar{\omega} = 0.2$, $\beta = 0.3$, $\alpha_o = 10°$ and $U_N^*/U_L^* = 1.01$	22
9(a)	Variation of Amplitude of α with Number of Cycles for $\bar{\omega} = 0.2$, $\mu = 100$, $x_\alpha = 0.25$, $\beta = 0.3$ and $U_N^*/U_L^* = 0.9992$	23
9(b)	Variation of α with Number of Cycles for $\bar{\omega} = 0.2$, $\mu = 100$, $x_\alpha = 0.25$, $\beta = 0.3$ and $U_N^*/U_L^* = 1.0$	24
9(c)	Variation of Amplitude of α with Number of Cycles for $\bar{\omega} = 0.2$, $\mu = 100$, $x_\alpha = 0.25$, $\beta = 0.3$ and $U_N^*/U_L^* = 1.0008$	25
9(d)	Variation of Amplitude of α with Number of Cycles for $\bar{\omega} = 0.2$, $\mu = 100$, $x_\alpha = 0.25$, $\beta = 0.3$ and $U_N^*/U_L^* = 1.0024$	26
10	Variation of Limit-Amplitude α_A with Non-Linear to Linear Flutter Speed Ratio for $\bar{\omega} = 0.2$ and $\mu = 100$	27
11	Variation of Limit-Amplitude ξ_A with Non-Linear to Linear Flutter Speed Ratio for $\bar{\omega} = 0.2$ and $x_\alpha = 0.25$	28
12	Variation of Limit-Amplitude ξ_A with Non-Linear to Linear Flutter Speed Ratio for $\bar{\omega} = 0.2$ and $\mu = 250$	29
13	Variation of Limit-Amplitude α_A with Non-Linear to Linear Flutter Speed Ratio for $\mu = 100$ and $x_\alpha = 0.25$	30
14	Variation of Limit-Amplitude ξ_A with Non-Linear to Linear Flutter Speed Ratio for $\mu = 100$ and $x_\alpha = 0.25$	31

APPENDICES

Appendix		Page
A		33
B		39

SYMBOLS

Symbol	Definition
$\bar{A}$	defined in Equation (A2)
a	constant in Equation (10)

SYMBOLS (Cont'd)

Symbol	Definition
a_h	non-dimensional distance measured from airfoil mid-chord to elastic axis
b	semi-chord of airfoil, also constant in Equation (10)
C_L	sectional aerodynamic lift coefficient
C_M	sectional aerodynamic pitching moment coefficient
c	chord, also constant in Equation (10)
d	constant in Equation (10)
$\bar{E}$	defined in Equation (A1)
h	plunge displacement
$\bar{I}$	defined in Equation (A3)
I_α	defined in Equation (17)
I_ξ	defined in Equation (16)
k	reduced frequency, $\frac{\omega b}{U}$
ℓ	constant in Equation (10)
$\bar{M}$	defined in Equation (A4)
m	mass of airfoil per unit span
P	external applied force
p	defined in Equation (6)
Q	external applied moment
r	defined in Equation (7)
r_α	radius of gyration about elastic axis
$\bar{T}$	defined in Equation (A7)
t	time
U	free stream velocity
$\bar{U}$	defined in Equation (A10)

SYMBOLS (Cont'd)

Symbol	Definition
U^*	non-dimensional velocity defined in Equation (5)
U_L^*	non-dimensional linear flutter speed
U_N^*	non-dimensional non-linear flutter speed
x_α	non-dimensional distance measured from elastic axis to centre of mass
α	pitch angle
α_A	limit-amplitude of α
β	coefficient of the non-linear term α^3
ζ_α	viscous damping for pitching motion
ζ_ξ	viscous damping for plunging motion
θ	coefficient of the non-linear term ξ^3
λ_α	defined in Equation (A8)
λ_ξ	defined in Equation (A9)
μ	airfoil-air mass ratio, $= m/\pi\rho b^2$
ξ	non-dimensional displacement
ξ_A	limit amplitude of ξ
ρ	air density
σ_α	defined in Equation (A5)
σ_ξ	defined in Equation (A6)
τ	non-dimensional time
ϕ	Wagner function
ψ^n, ψ_2^n	defined in Appendix B
ω	frequency
ω_α	uncoupled natural frequency of pitching motion
ω_ξ	uncoupled natural frequency of plunging motion

SYMBOLS (Cont'd)

Symbol	Definition
$\bar{\omega}$	ratio, $\frac{\omega_\xi}{\omega_\alpha}$

Subscripts

o	initial conditions

1.0 Introduction

In aeroelastic investigations, it is generally assumed that the structural behaviour of an aircraft is linear. Flutter analysis of two and three-dimensional airfoils using linear theory is a well known subject (Refs. 1,2). However, in reality non-linearities are present in one form or the other. Structurally, they may occur in the restoring forces and can be treated as non-linear springs, for example, springs with free play, hysteresis or cubic non-linearities. These types of non-linearities have been investigated by Woolston et al (Ref. 3) for a two-dimensional airfoil performing pitching and plunging motions using an analog computer. There are serious drawbacks in the use of an analog computer to study non-linear flutter and accuracy is often not as great as one would desire.

An alternate approach was suggested by Shen (Ref. 4) using the well known Kryloff and Bogoliuboff (Ref. 5) method in non-linear vibration theory. The original limitation of weak non-linearities can be removed by adopting a modification given by Popov (Ref. 6). The analysis assumes the existence of a periodic solution dominated by the fundamental harmonic. The amplitude of oscillation in the degree of freedom which contains the non-linearity is prescribed and the critical velocity at which the specified oscillation will be sustained is then determined. It has not been demonstrated how large the magnitude of the non-linearities is admissible and how the effects of initial conditions on the flutter boundary can be accounted for.

This report describes a method for non-linear flutter analysis that eliminates the limitations inherent in the earlier methods (Refs. 3 and 4) by the use of a time marching finite difference

scheme. The use of numerical time marching techniques in aeroelastic studies was first reported by Ballhaus and Goorjian (Ref. 7) who investigated the response of a NACA 64A006 airfoil with a single-degree-of-freedom in pitch at transonic speeds. Extensions of this procedure to two- and three-degree-of-freedom have been reported by Rizzetta (Ref. 8) and Yang and Chen (Ref. 9). Only a linear response was treated by these authors. Numerical methods applied to non-linear vibration problems have received little attention until recently. A study has been made by Lee and LeBlanc (Ref. 10) which deals with the effect of non-linear aerodynamic loads on the dynamic response of a two-dimensional airfoil performing pitching and plunging oscillations. For a one-degree-of-freedom system with cubic restoring force in the absence of aerodynamic loads, Jones and Lee (Ref. 11) investigated the multivalued response curve of amplitude versus frequency and showed the effects of initial conditions on the steady state of the system under forced oscillations.

There exists a number of numerical time marching techniques developed for finite element linear structural analysis. Among the most commonly used time integration schemes are the explicit central difference technique and Houbolt's, Wilson's and Newmark's methods (Ref. 12,13). Except for the explicit scheme, the other three methods are unconditionally stable. Higher order schemes are also discussed in Ref. 11 and they are conditionally stable. Provided that care is taken to chose a time step sufficiently small to ensure the highest mode considered in a vibrating system does not diverge, higher order

schemes are more efficient in terms of computation time. However, for a system with few structural components or the number of vibration modes is small, higher order methods such as the eighth order scheme reported in Ref. 11 does not offer any distinct advantage over Houbolt's scheme which is simpler and less cumbersome to use. For this reason, Houbolt's method is adopted in this investigation.

Using incompressible aerodynamics, the aeroelastic equations for a two-dimensional airfoil performing plunging and pitching motions are written as a pair of simultaneous cubic equations in finite difference form. Without loss in generality, the elastic axis is assumed to be located at the airfoil's 1/4 chord. This simplifies the algebra in the derivation of the finite difference equations considerably. Only cubic non-linear restoring force in the pitch degree of fredom is considered. Other types of non-linearities can be treated in the same manner numerically. The effect of initial conditions on non-linear flutter is studied by varying the displacement from equilibrium of the pitch angle at the start of the airfoil motion. Divergent flutter for soft springs and limit-cycle flutter for hard springs are investigated from case studies using various airfoil parameters and coefficients of the non-linear term in the restoring force.

2.0 Analysis

2.1 Two-Degree-of-Freedom Motion of a 2-D Airfoil

Figure 1 shows the notations used in the analysis of a two-degree-of-freedom motion of an airfoil oscillating in pitch and in

plunge. The plunging deflection is denoted by h, positive in the downward direction, α is the pitch angle about the elastic axis, positive with the nose up. The elastic axis is located at a distance $a_h b$ from the midchord, while the mass centre is located at a distance $x_\alpha b$ from the elastic axis. Both distances are positive when measured towards the trailing edge of the airfoil. The aeroelastic equations of motion for linear springs have been derived by Fung (Ref. 2). For non-linear restoring forces such as those for cubic springs considered in this report, they can be written as follows:

$$\xi'' + x_\alpha \alpha'' + 2\zeta_\xi \frac{\bar{\omega}}{U^*} \xi' + \left(\frac{\bar{\omega}}{U^*}\right) \left(\xi + \theta \xi^3\right) = p(\tau) \qquad (1)$$

$$\frac{x_\alpha}{r_\alpha^2} \xi'' + \alpha'' + 2\zeta_\alpha \frac{\alpha'}{U^*} + \frac{1}{U^{*2}} \left(\alpha + \beta\zeta^3\right) = r(\tau) \qquad (2)$$

where $\xi = h/b$ is the non-dimensional displacement and the ' denotes differentiation with respect to the non-dimensional time τ defined as

$$\tau = \frac{Ut}{b} \qquad (3)$$

In Eqs. (1) and (2), $\bar{\omega}$ is given by

$$\bar{\omega} = \frac{\omega_\xi}{\omega_\alpha} \qquad (4)$$

where ω_ξ and ω_α are the uncoupled plunging and pitching natural frequencies. ζ_ξ and ζ_α are the viscous damping ratio for plunge and pitch respectively, r_α is the radius of gyration about the elastic axis, θ and β are the non-linear spring constants. U^* is defined as

$$U^* = \frac{U}{b\omega_\alpha} \qquad (5)$$

and

$$p(\tau) = -\frac{1}{\pi\mu} C_L(\tau) + \frac{P(\tau)b}{mU^2} \qquad (6)$$

$$r(\tau) = \frac{2}{\pi\mu r_\alpha^2} C_M(\tau) + \frac{Q(\tau)}{mU^2 r_\alpha^2} \tag{7}$$

where $C_L(\tau)$ and $C_M(\tau)$ are the lift and pitching moment coefficient respectively. $P(\tau)$ and $Q(\tau)$ are the external applied force and moment respectively, m is the airfoil mass per unit span and μ the airfoil-air mass ratio.

For incompressible flow, Fung (Ref. 2) gives the following expressions for $C_L(\tau)$ and $C_M(\tau)$:

$$C_L(\tau) = \pi (\xi'' - a_h\alpha'' + \alpha') + 2\pi \left[\left[\alpha(0) + \xi'(0) + (\tfrac{1}{2}-a_h)\ \alpha'(0)\right]\phi(\tau) + \int_0^\tau \phi(\tau - \sigma)\ (\alpha'(\sigma) + \xi''(\sigma) + (\tfrac{1}{2} - a_h)\ \alpha''(\sigma))d\sigma\right] \tag{8}$$

$$C_M(\tau) = (\tfrac{1}{2} + a_h)\pi\left[(\alpha(0) + \xi'(0) + (\tfrac{1}{2} - a_h)\alpha'(0))\phi(\tau) + \int_0^\tau \phi(\tau - \sigma)\ (\alpha'(\sigma) + \xi''(\sigma) + (\tfrac{1}{2} - a_h)\alpha''(\sigma))d\sigma\right] + \frac{\pi}{2} a_h\ (\xi'' - a_h\alpha'') - (\tfrac{1}{2} - a_h)\frac{\pi}{2}\alpha' - \frac{\pi}{16}\alpha'' \tag{9}$$

where the Wagner function $\phi(\tau)$ is given by

$$\phi(\tau) = \ell - ae^{-b\tau} - ce^{-d\tau} \tag{10}$$

and the constants $\ell = 1$, $a = 0.165$, $b = 0.0455$, $c = 0.335$ and $d = 0.3$.

2.2 Finite Difference Scheme

Houbolt's (Ref. 13) implicit method is used in the present analysis. The derivatives at time $\tau+\Delta\tau$ are replaced with backward difference formulas using values at three previous points. For example,

$$\alpha''_{\tau+\Delta\tau} = \frac{1}{\Delta\tau^2}\left(2\alpha_{\tau+\Delta\tau} - 5\alpha_\tau + 4\alpha_{\tau-\Delta\tau} - \alpha_{\tau-2\Delta\tau}\right) + O(\Delta\tau^2) \tag{11}$$

and

$$\alpha'_{\tau+\Delta\tau} = \frac{1}{6\Delta\tau}\left(11\ \alpha_{\tau+\Delta\tau} - 18\alpha_\tau + 9\alpha_{\tau-\Delta\tau} - 2\alpha_{\tau-2\Delta\tau}\right) + O(\Delta\tau^3) \tag{12}$$

Similar expressions can be written for $\xi''_{\tau+\Delta\tau}$ and $\xi'_{\tau+\Delta\tau}$. In difference form, Eqs. (1) and (2) can be written as

$$\bar{I}\alpha_{\tau+\Delta\tau} + \bar{M}\xi_{\tau+\Delta\tau} + \left(\frac{\bar{\omega}}{U^*}\right)^2 \theta\xi^3_{\tau+\Delta\tau} = \bar{U} \tag{13}$$

$$\bar{E}\,\xi_{\tau+\Delta\tau} + \bar{A}\alpha_{\tau+\Delta\tau} + \frac{\beta}{U^{*2}}\,\alpha^3_{\tau+\Delta\tau} = \bar{T} \tag{14}$$

The coefficients $\bar{E}$, $\bar{A}$, $\bar{I}$, $\bar{M}$ and the terms $\bar{U}$ and $\bar{T}$ on the RHS of Eqs. (13) and (14) are given in the Appendix A. The derivation is for $a_h = -\frac{1}{2}$, that is, for location of the elastic axis at the $\frac{1}{4}$ chord.

2.3 Recurrence Formula for Aerodynamic Lift

For $a_h = -\frac{1}{2}$, Eq. (9) reduces to a rather simple form and only the expression for C_L involves an integration at each time step. To reduce the amount of computations, a recurrence formula is derived. The lift coefficient in Eq. (8) can be written as

$$C_L(\tau) = \pi(\xi'' + \tfrac{1}{2}\alpha'' + \alpha') + 2\pi\left[\{\alpha(0) + \xi'(0) + \alpha'(0)\}\phi(\tau) + I_\xi(\tau) + I_\alpha(\tau)\right] \tag{15}$$

where

$$I_\xi(\tau) = \int_0^\tau \xi''(\sigma)\phi(\tau - \sigma)d\sigma \tag{16}$$

and

$$I_\alpha(\tau) = \int_0^\tau (\alpha''(\sigma) + \alpha'(\sigma))\phi(\tau - \sigma)d\sigma \tag{17}$$

Substituting Eq. (10) into Eqs. (16) and (17), and using Simpson's rule $I_\xi(\tau+\Delta\tau)$ and $I_\alpha(\tau+\Delta\tau)$ can be written as

$$I_\xi(\tau+\Delta\tau) = I_\xi(\tau) + \sigma_\xi\xi_{\tau+\Delta\tau} + \lambda_\xi \tag{18}$$

$$I_\alpha(\tau+\Delta\tau) + I_\alpha(\tau) + \sigma_\alpha\alpha_{\tau+\Delta\tau} + \lambda_\alpha \tag{19}$$

where σ_α, σ_ξ, λ_α and λ_ξ are defined by Eqs. (A5), (A6), (A8) and (A9) in the Appendix A. Using Eqs. (18) and (19), $C_L(\tau+\Delta\tau)$ can readily be computed.

2.4 Starting Procedure

Houbolt's scheme requires values of α and ξ at times $\tau-2\Delta\tau$, $\tau-\Delta\tau$ and τ in order to determine their values at $\tau+\Delta\tau$. At time $\tau = 0$, a special starting procedure is required. A Taylor series is used to obtain the following:

$$\alpha_{-\Delta\tau} = \alpha_o - \Delta\tau\alpha_o' + \frac{\Delta\tau^2}{2}\alpha_o'' + O(\Delta\tau^3) \tag{20}$$

$$\alpha_{\Delta\tau} = \alpha_o + \Delta\tau\alpha_o' + \frac{\Delta\tau^2}{2}\alpha_o'' + O(\Delta\tau^3) \tag{21}$$

with similar expressions for $\xi_{-\Delta\tau}$ and $\xi_{\Delta\tau}$. The expressions for C_L and C_M involves the first and second derivatives of α and ξ, and these derivatives are obtained as follows:

$$\alpha'_{-\Delta\tau} = \alpha_o' - \Delta\tau\alpha_o'' + \frac{\Delta\tau^2}{2}\alpha_o''' + O(\Delta\tau^3) \tag{22}$$

$$\alpha'_{\Delta\tau} = \alpha_o' + \Delta\tau\alpha_o'' + \frac{\Delta\tau^2}{2}\alpha''' + O(\Delta\tau^3) \tag{23}$$

and

$$\alpha''_{-\Delta\tau} = \alpha_o'' - \Delta\tau\alpha_o''' + \frac{\Delta\tau^2}{2}\alpha_o^{Iv} + O(\Delta\tau^3) \tag{24}$$

$$\alpha''_{\Delta\tau} = \alpha_o'' + \Delta\tau\alpha_o''' + \frac{\Delta\tau^2}{2}\alpha_o^{Iv} + O(\Delta\tau^3) \tag{25}$$

with expressions for the ξ derivatives written in the same form as those given in Eqs. (22) to (25). The initial conditions α_o, α_o', ξ_o and ξ_o' are known and the higher derivatives can be obtained from Eqs. (1) and (2) and are given by

$$\left(1 + \frac{1}{\mu}\right)\frac{d^n\xi_o}{d\tau^n} + \left(x_\alpha + \frac{1}{2\mu}\right)\frac{d^n\alpha_o}{d\tau^n} = \psi_1^n \tag{26}$$

$$\frac{1}{r_\alpha^2}\left(x_\alpha + \frac{1}{2\mu}\right)\frac{d^n\xi_o}{d\tau^n} + \left(1 + \frac{3}{8\mu r_\alpha^2}\right)\frac{d^n\alpha_o}{d\tau^n} = \psi_2^n \tag{27}$$

where $n = 2,3,4$ and ψ_1^n, ψ_2^n are given in Appendix B. For the next step, Houbolt's scheme can be used since α and ξ at $\tau = -\Delta\tau, 0$ and $\Delta\tau$ are known. The accuracy of the numerical method is $O(\Delta\tau^4)$ on each step

while Eqs. (20) to (25) limit the accuracy to $O(\Delta\tau^3)$. A starting accuracy higher than $O(\Delta\tau^3)$ is not necessary since the error per cycle in the numerical scheme is $\frac{2\pi}{\omega} O(\Delta\tau^3)$ (Ref. 11).

3.0 Results and Discussions

As mentioned in the Introduction, only non-linearities in the pitch degree of freedom is considered. Hence θ in Eq. (1) is set equal to zero and Eqs. (13) and (14) can be combined to form a single cubic equation. In flutter analysis, $P(\tau)$ and $Q(\tau)$ are set to zero. The elastic axis of the airfoil is placed at the $\frac{1}{4}$ chord location (that is, $a_h = -0.5$) and r_α is kept at a value of 0.5. Other properties of the airfoil, such as, μ, x_α, $\bar{\omega}$ and β are varied.

3.1 Flutter Boundaries for Soft Spring

For a soft spring, β is negative. The deviation from linearity of the restoring spring force is shown in Fig. 2 where the term $\alpha + \beta\alpha^3$ in Eq. (2) is plotted against α for various β. Values of β up to ± 3 are considered in this report.

In determining the flutter boundary for a given set of values for μ, x_α, $\bar{\omega}$ and β, Eqs. (13) and (14) are solved for known initial conditions. Throughout this study, it is assumed that $\xi_o = \xi_o' = \alpha_o' = 0$ and only α_o changes. The procedure then is to determine the linear flutter speed first. For given α_o, a value of U^* smaller than the linear flutter speed is selected and α and ξ are obtained by the time marching finite difference scheme. The flutter speed is determined when the solution is neutrally stable, and the boundary is given by the α_o versus flutter speed curve. Figure 3 illustrates the behaviour of α

with time in the stable and unstable regions. The value of $\mu = 100$, $x_\alpha = 0.25$, $\bar{\omega} = 0.2$, $\bar{\beta} = -3.0$ and $\alpha_o = 10°$. The non-dimensional flutter speeds, expressed as ratios of the non-linear to linear flutter speed, are 0.96 and 0.973 respectively.

In numerical time integration schemes, Bathe and Wilson (Ref. 12) pointed out that the amplitude decays due to numerical errors and is dependent on the time step $\Delta\tau$. The value of $\Delta\tau$ is taken to be 1/256 of the shorter period of the two coupled modes of oscillation in the absence of aerodynamic forces. The periods of the coupled modes are obtained from solving Eqs. (1) and (2) for $\beta = \theta = p(\tau) = r(\tau) = 0$. This value of $\Delta\tau$ is found to be sufficiently small to give good accuracies in determining the flutter boundaries while ensuring the computation time is not excessive.

The destabilizing effect of a soft spring is illustrated in Fig. 4 which shows the flutter boundaries for three values of $\beta = -0.3$, -1.0 and -3.0. The airfoil has the following properties: $x_\alpha = 0.25$ and $\bar{\omega} = 0.2$ while r_α and a_h, as stated at the beginning of this section, retain the values of 0.5 and -0.5 respectively throughout this investigation. For a given value of β, the flutter region lies to the right of the boundary curve and it is seen that flutter can be induced below the linear flutter speed by increasing the initial displacement α_o. In the vicinity of the flutter boundary, the rate at which the oscillation decays or diverges, depending whether U* is to the left or right of the boundary, usually increases with increasing α_o and/or decreasing β.

Of the various parameters that affect the flutter boundary, only μ, $\bar{\omega}$ and x_α are being investigated. Figure 4 shows that increasing μ has a destabilizing effect and the boundary curves are all displaced to the left. The effect is more pronounced as the value of β decreases.

Increasing the distance between the centre of mass and the elastic axis has a stabilizing effect. Comparing the curves in Fig. 4 for $\mu = 250$ with Figs. 5 and 6 shows the flutter boundaries move closer to the linear flutter speed as x_α is increased. Finally, the effect of $\bar{\omega}$ can be observed by comparing the curves in Figs. 7 and 4. As the uncoupled natural frequency for plunging motion approaches that for pitching motion, the flutter boundaries move towards that for the linear case. When $\bar{\omega}$ reaches a value of 1.2, it is seen that the flutter boundaries are virtually independent on the coefficient β.

3.2 Limit-Cycle Flutter for Hard Spring

For positive values of β (hard spring), divergent flutter is not encountered. Instead, the flutter boundaries for all β coalesce into a straight line at the linear flutter speed. To the right of this boundary, the oscillation is self-excited and maintains a constant amplitude which is self-limited. Figure 8 shows the typical behaviour of α in the stable and limit-cycle flutter regions. The value of $\mu = 100$, $x_\alpha = 0.25$, $\bar{\omega} = 0.2$, $\bar{\beta} = -3.0$ and $\alpha_o = 10°$ are chosen in this example. The non-linear to linear flutter speed ratios are 0.99 and 1.01 respectively. For speed ratios not very close to unity, the time it takes for the oscillations to decay to zero or to reach a steady

state amplitude is usually quite short. However, if the solution is required very close to the flutter boundary, a large number of cycles has to be computed. This is illustrated in Fig. 9 for $\bar{\omega} = 0.2$, $\mu = 100$, $x_\alpha = 0.25$ and $\beta = 0.3$ for four values of the speed ratio U_N^*/U_L^*. For $U_N^*/U_L^* > 1$, the curves with different initial displacement α_o coalesce, indicating the final amplitude attained when steady conditions are reached to be independent of α_o. At $U_N^*/U_L^* = 1$, the curves converge very slowly, often requiring a large number of cycles to be computed before the solution gives a constant amplitude. However, a small increase in U_N^*/U_L^* shows a sharp decrease in the number of computation cycles required as illustrated in Figs. 9c and 9d.

For the degree of freedom with the non-linearity present, which is the α oscillation in this case, the limit-amplitude oscillation for fixed r_α and a_h is a function of velocity, $\bar{\omega}$, β and x_α. It is shown in Fig. 10 for $\bar{\omega} = 0.2$ and $\mu = 100$ that the limit-amplitude α_A increases with increasing x_α. Computations for $\mu = 50$ and 250 give identical curves. The other degree of freedom ξ shows a dependence on μ and Fig. 11 indicates that the amplitude ξ_A increases with increasing μ. The variation of ξ_A with x_α is given in Fig. 12. Unlike α_A, ξ_A decreases with increasing x_α.

The final parameter to consider is $\bar{\omega}$. Figures 13 shows an increase of α_A with increasing $\bar{\omega}$. Comparing Fig. 14 with the curve for $\mu = 100$ in Fig. 11 shows that between the range of $\bar{\omega} = 0.2$ to 0.8, there is a large decrease in ξ_A while Fig. 13 shows the corresponding value of α_A increases only slightly.

4.0 Conclusions

Flutter analysis of a two-dimensional airfoil with cubic non-linear restoring force in the pitch degree of freedom is studied using a numerical time marching finite difference scheme. For a soft spring, flutter can be induced below the linear flutter speed by increasing the intial displacement from equilibrium of the pitch angle. Factors that have a destabilizing effect are an increase in the coefficient of the non-linear term in the restoring force, an increase in the airfoil-air mass ratio. Increasing the distance between the centre of mass and the elastic axis or the ratio of the plunge to pitch natural frequencies moves the flutter boundaries closer to the linear case and hence has a stabilizing effect.

For a hard spring, divergent flutter is not encountered. Instead, the oscillations maintain a self-limited amplitude which is independent of the initial angular displacement. In the pitch degree of freedom which contains the non-linearity, the amplitude does not depend on the airfoil-air mass ratio, while the plunge amplitude increases with an increase in that ratio. Increasing the distance between the centre of mass and elastic axis results in a larger pitch amplitude while the plunge amplitude gets smaller. As the ratio of the uncoupled natural frequencies of the plunge to pitch motion approaches and exceeds unity, there is an increase in the pitch amplitude while a large drop in the plunge amplitude is detected.

5.0 References

1. Bisplinghoff, R.L. Ashley, H. and Halfman, R.L. — Aeroelasticity, Addison-Wesley Publishing, Cambridge, Mass., 1955.

2. Fung, Y.C. — An Introduction to the Theory of Aeroelasticity, John Wiley and Sons, N.Y., 1955.

3. Woolston, D.S. Runyan, H.L. and Andrews, R.E. — An Investigation of Certain Types of Structural Nonlinearities on Wing and Control Surface Flutter, Journal Aeronautical Sciences, Vol. 24, No. 1, pp. 57-63, 1957.

4. Shen, S.F. — An Approximate Analysis of Nonlinear Flutter Problems, Journal Aeronautical Sciences, Vol. 26, No. 1, pp. 25-32, 1959.

5. Kryloff, N. and Bogoliuboff, N. — Introduction to Nonlinear Mechanics, Translation by Solomon Lifschitz, Princeton University Press, Princeton, 1947.

6. Popov, E.P. — On the Use of the Harmonic Linearization Method in Automatic Control Theory, NACA TM1406, Jan. 1957.

7. Ballhaus, W.F. and Goorjian — Computation of Unsteady Transonic Flows by the Indicial Method, AIAA Journal, Vol. 16, No. 2, pp. 117-124, 1978.

8. Rizzetta, D.P. — Time Dependent Response of a Two-Dimensional Airfoil in Transonic Flow, AIAA Journal, Vol. 17, No. 1, pp. 26-32, 1979.

9. Yang, T.Y. and Chen, C.H. — Transonic Flutter and Response Analysis of Two Three-Degree-of-Freedom Airfoils, J. Aircraft, Vol. 19, No. 10, pp. 872-884, 1982.

10. Lee, B.H.K. and LeBlanc, P. — Forced Oscillation of a Two-Dimensional Airfoil with Non-Linear Aerodynamic Loads, National Research Council Canada, LR-617, 1985.

11. Jones, D.J. and Lee, B.H.K. — Time Marching Numerical Solution of the Dynamic Response of Non-Linear Systems, National Research Council Canada, NAE-AN-25, Jan. 1985.

12. Bathe, K.J. and Wilson, E.L. — Numerical Methods in Finite Element Analysis, Prentice-Hall Inc., Englewood Cliffs, New Jersey, 1976.

13. Houbolt, J.C. — A Recurrence Matrix Solution for the Dynamic Response of Elastic Aircraft, Journal Aeronautical Sciences, Vol. 17, No. 9, pp. 540-550, 1950.

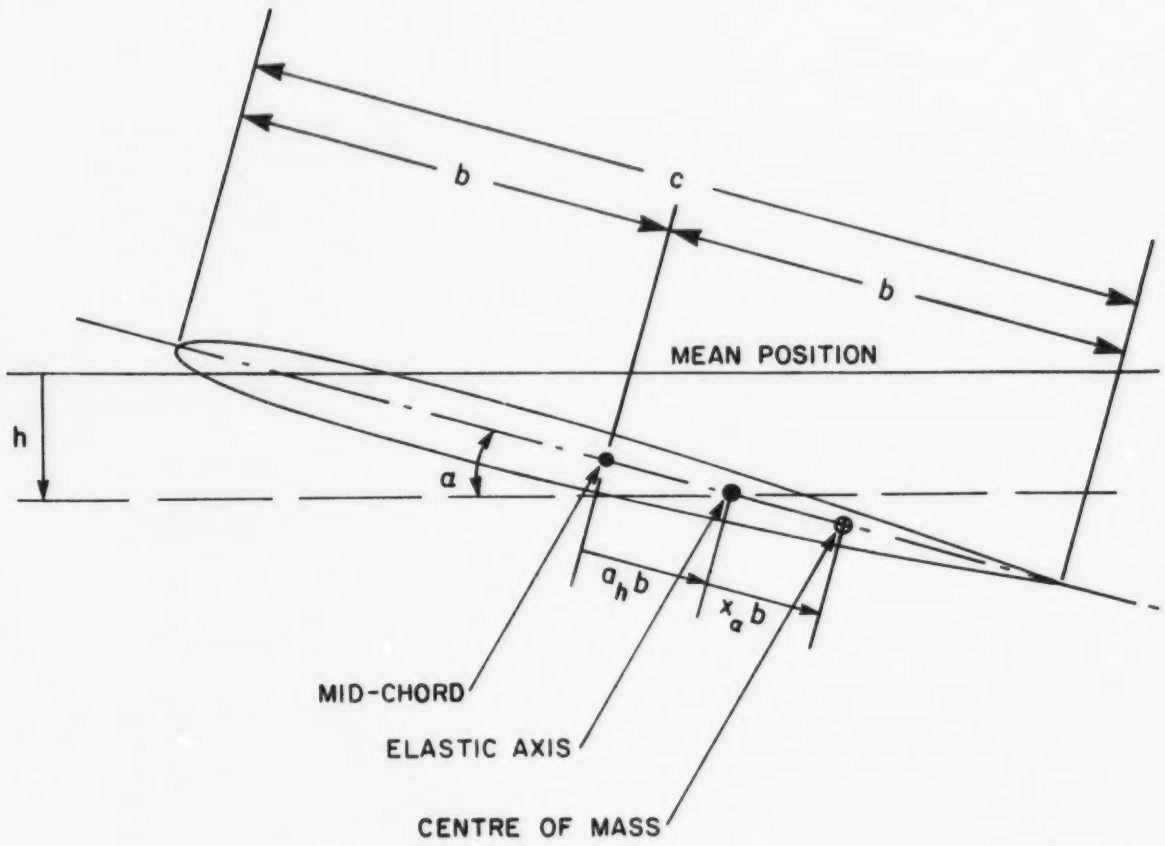

FIG. 1: TWO-DEGREE-OF-FREEDOM AIRFOIL MOTION

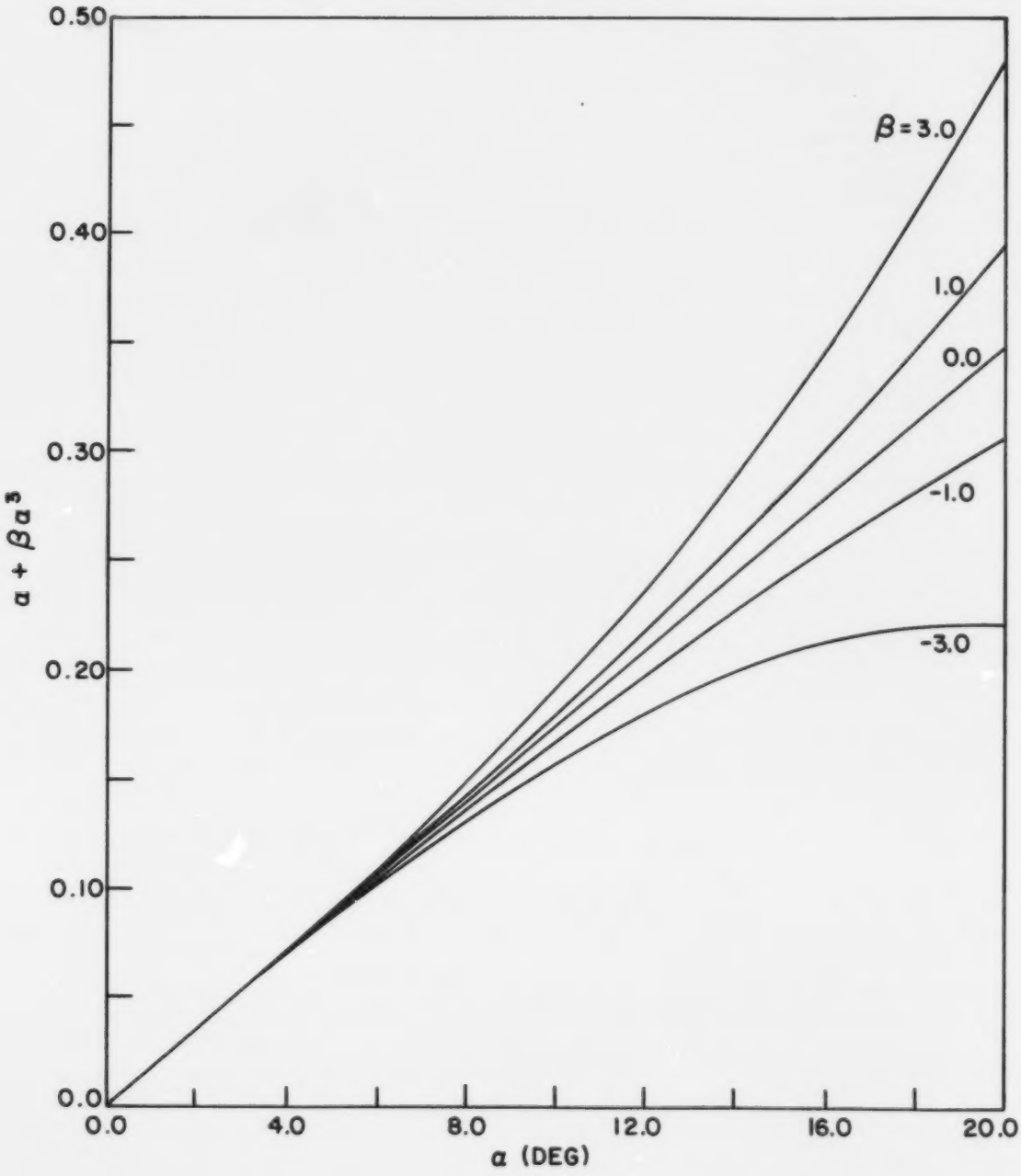

FIG. 2: EFFECT OF β ON NON-LINEAR RESTORING FORCE

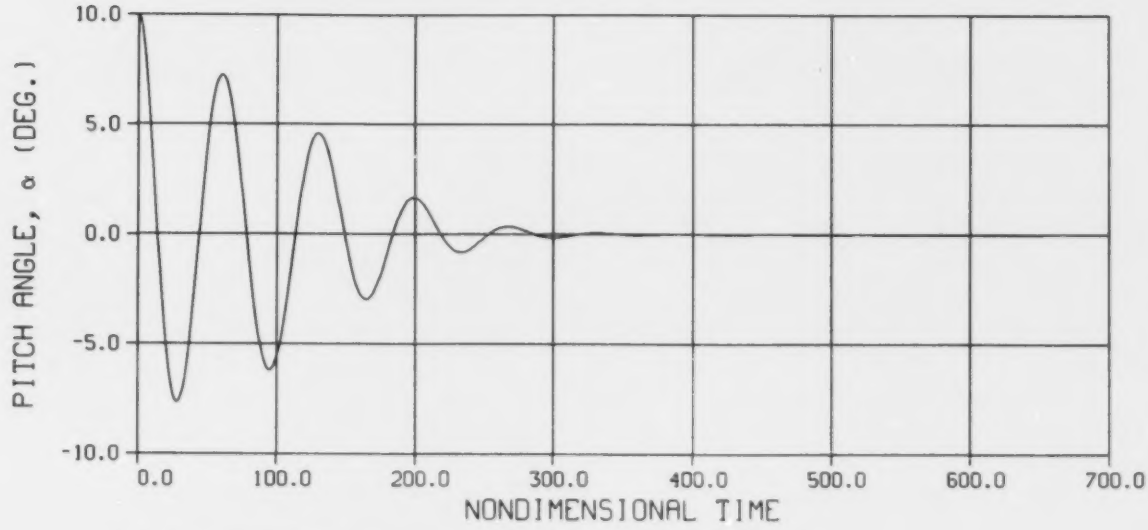

FIG. 3(a): TIME VARIATION OF α IN STABLE REGION FOR $\mu = 100$, $x_\alpha = 0.25$, $\bar{\omega} = 0.2$, $\beta = -3.0$, $\alpha_o = 10°$ AND $U_N^*/U_L^* = 0.96$

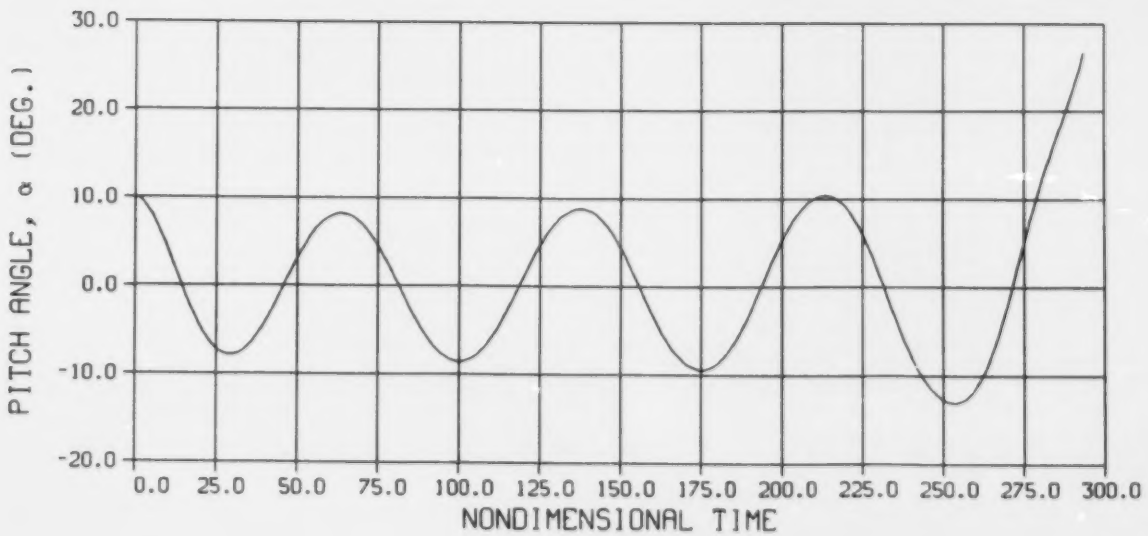

FIG. 3(b): TIME VARIATION OF α IN FLUTTER REGION FOR $\mu = 100$, $x_\alpha = 0.25$, $\bar{\omega} = 0.2$, $\beta = -3.0$, $\alpha_o = 10°$ AND $U_N^*/U_L^* = 0.973$

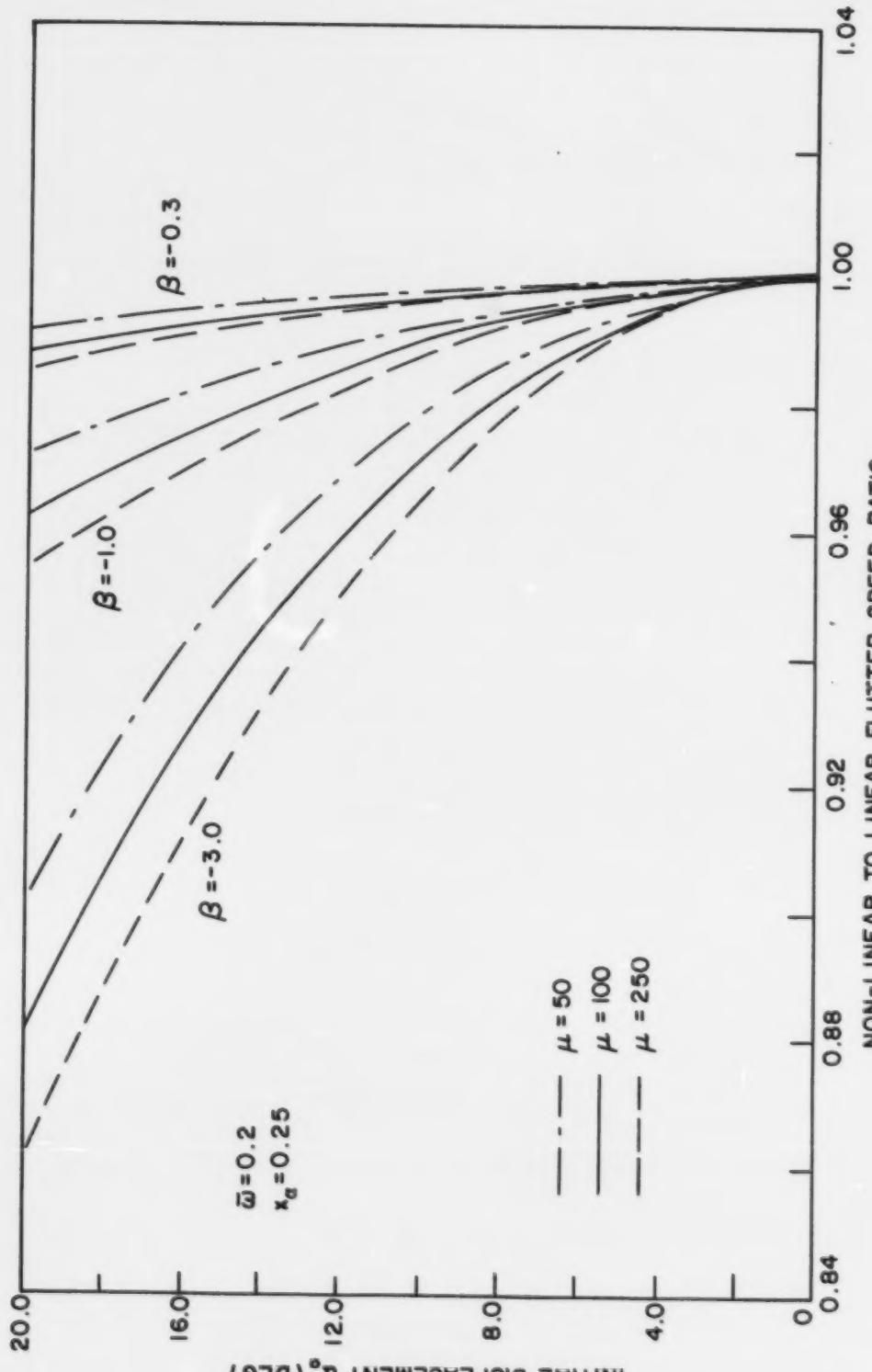

FIG. 4: EFFECT OF μ ON THE FLUTTER BOUNDARIES FOR $\bar{\omega} = 0.2$, $x_\alpha = 0.25$

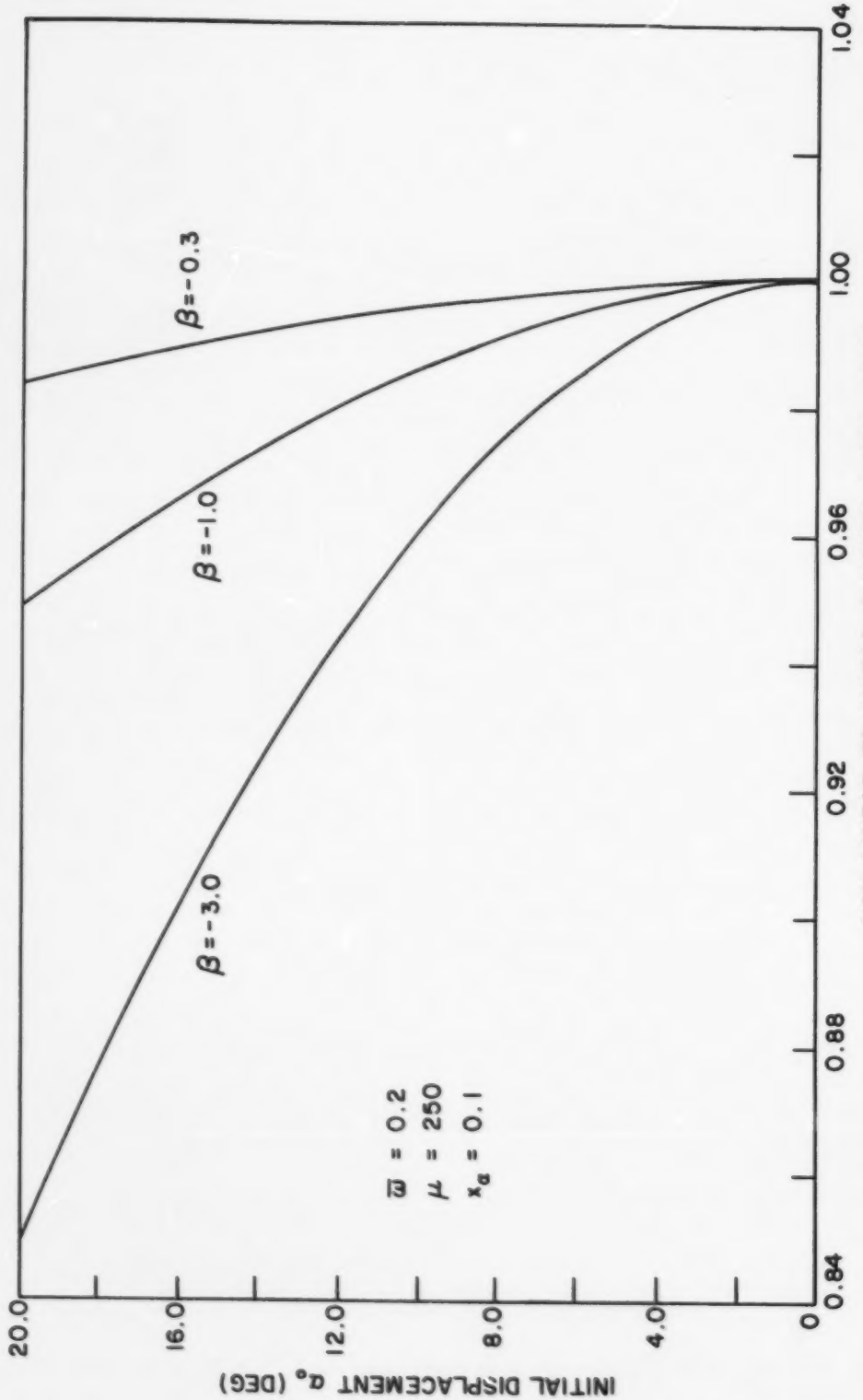

FIG. 5: FLUTTER BOUNDARIES FOR $\bar{\omega} = 0.2, \mu = 250$ AND $x_\alpha = 0.1$

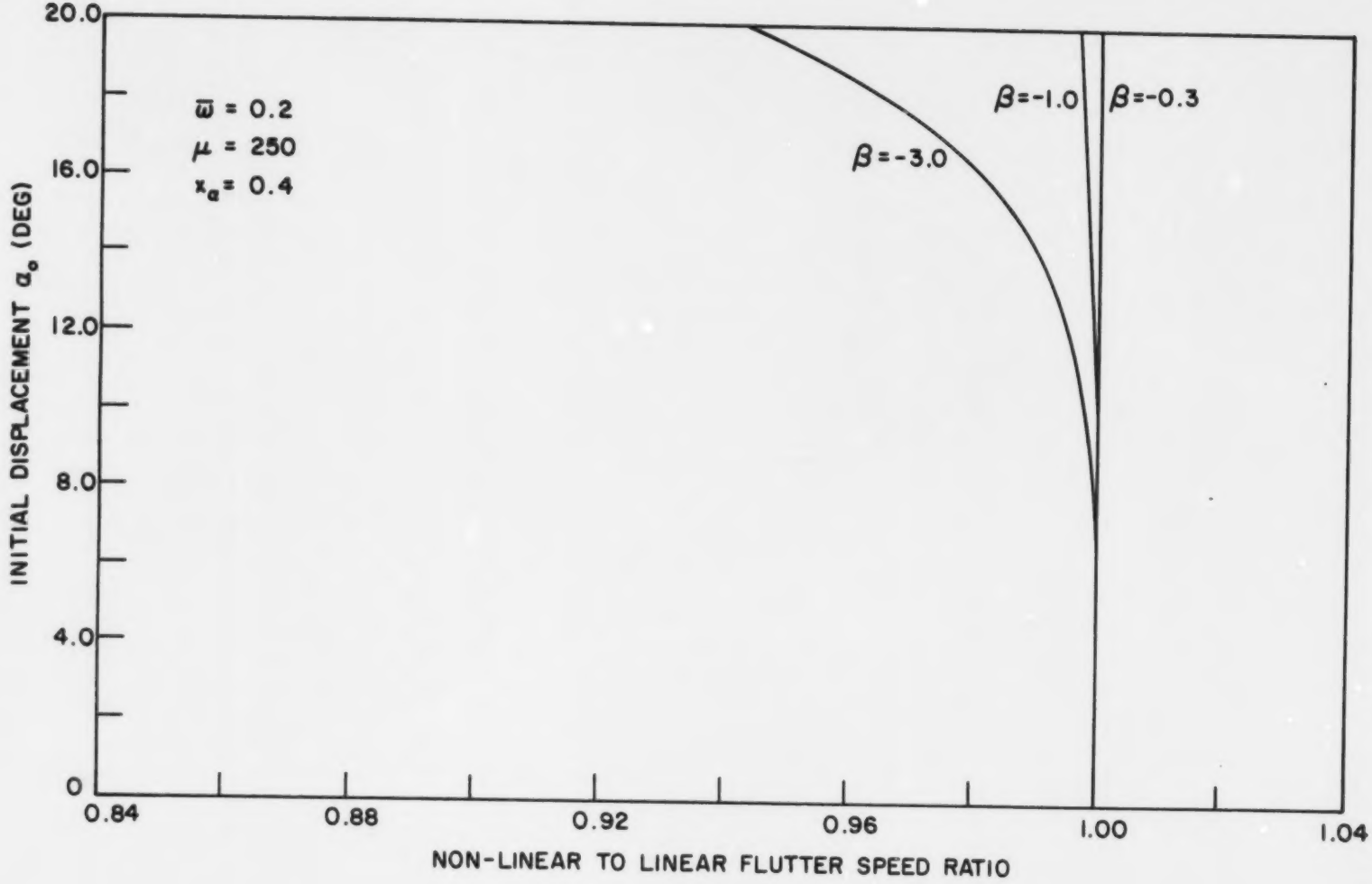

FIG. 6: FLUTTER BOUNDARIES FOR $\bar{\omega} = 0.2$, $\mu = 250$ AND $x_\alpha = 0.4$

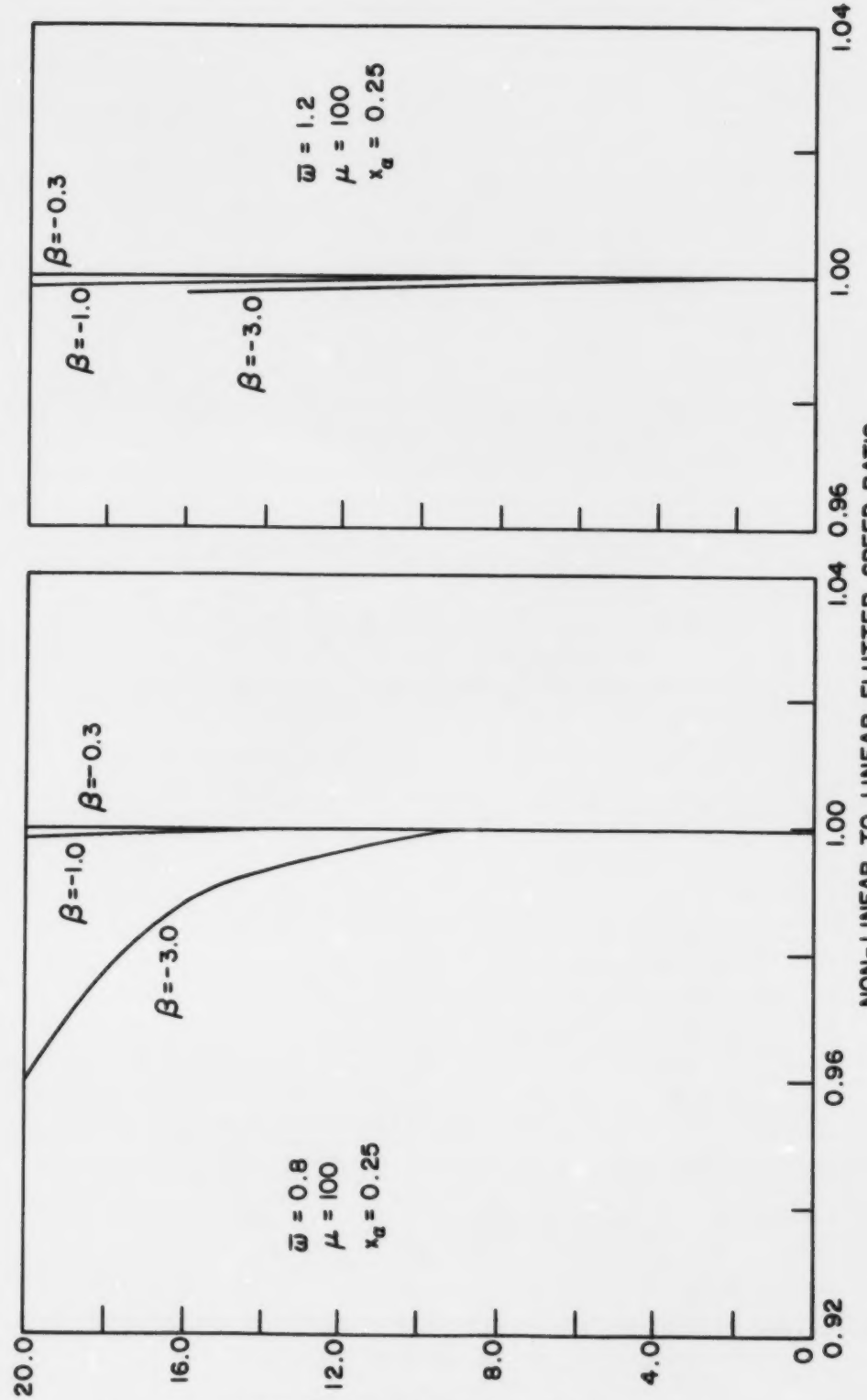

FIG. 7: FLUTTER BOUNDARIES FOR $\mu = 100$, $x_\alpha = 0.25$, $\bar{\omega} = 0.8$ AND 1.2

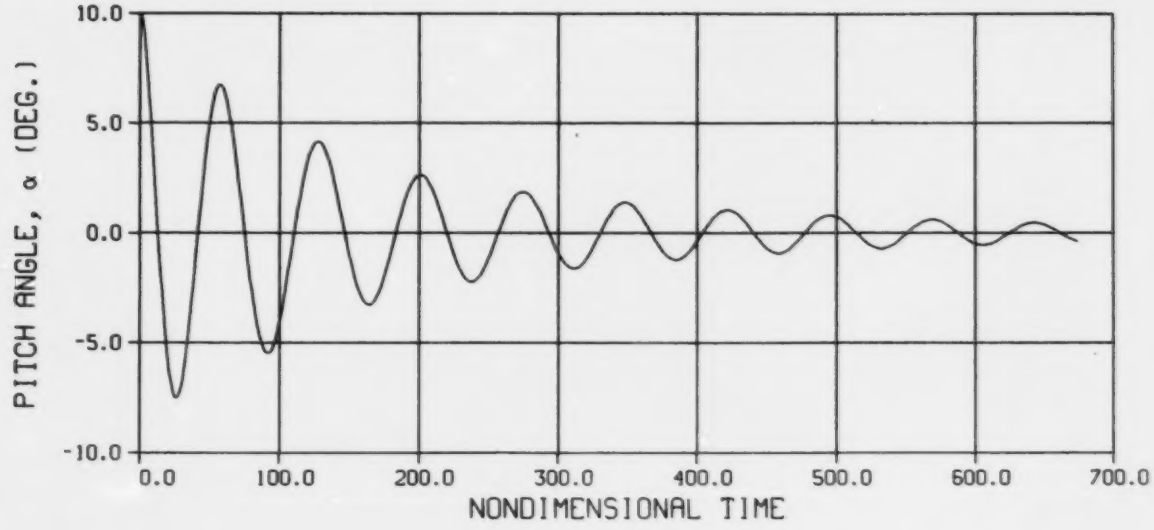

FIG. 8(a): TIME VARIATION OF α IN STABLE REGION FOR $\mu = 100$, $x_\alpha = 0.25$, $\bar{\omega} = 0.2$, $\beta = 0.3$, $\alpha_o = 10°$ AND $U_N^*/U_L^* = 0.99$

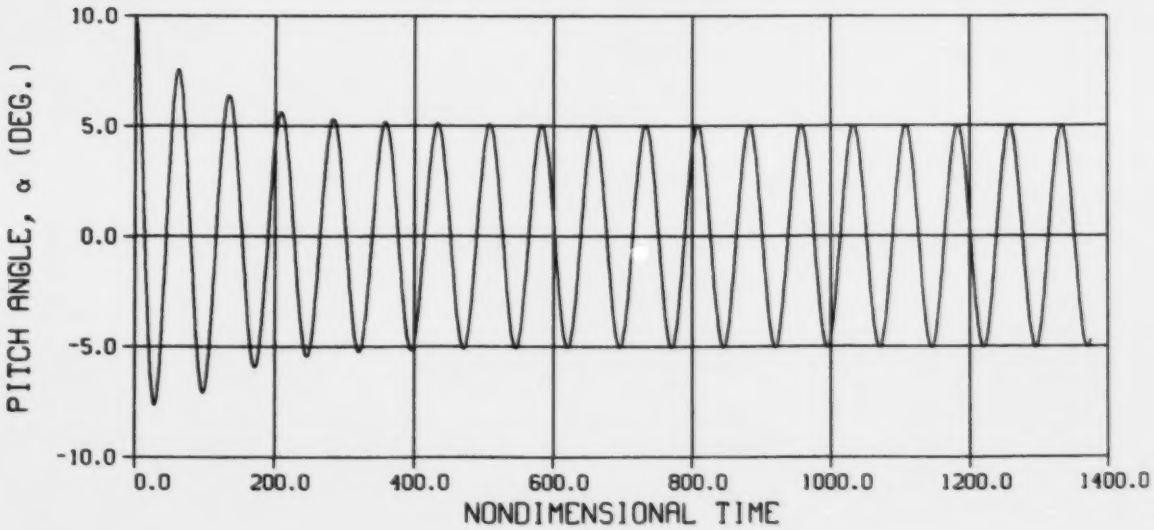

FIG. 8(b): TIME VARIATION OF α IN FLUTTER REGION FOR $\mu = 100$, $x_\alpha = 0.25$, $\bar{\omega} = 0.2$, $\beta = 0.3$, $\alpha_o = 10°$ AND $U_N^*/U_L^* = 1.01$

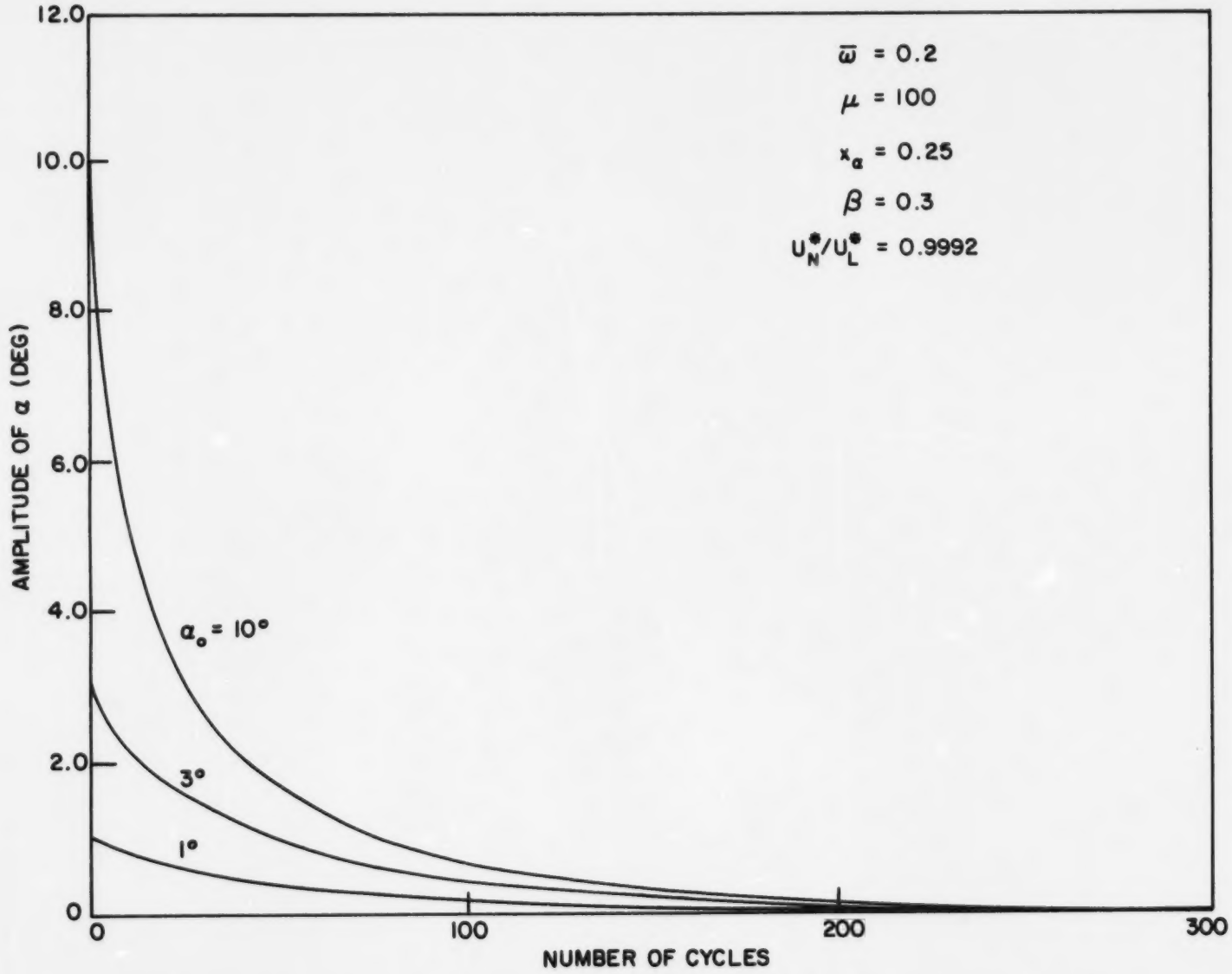

FIG. 9(a): VARIATION OF AMPLITUDE OF α WITH NUMBER OF CYCLES FOR $\bar{\omega}$ = 0.2, μ = 100, x_α = 0.25, β = 0.3 AND U_N^*/U_L^* = 0.9992

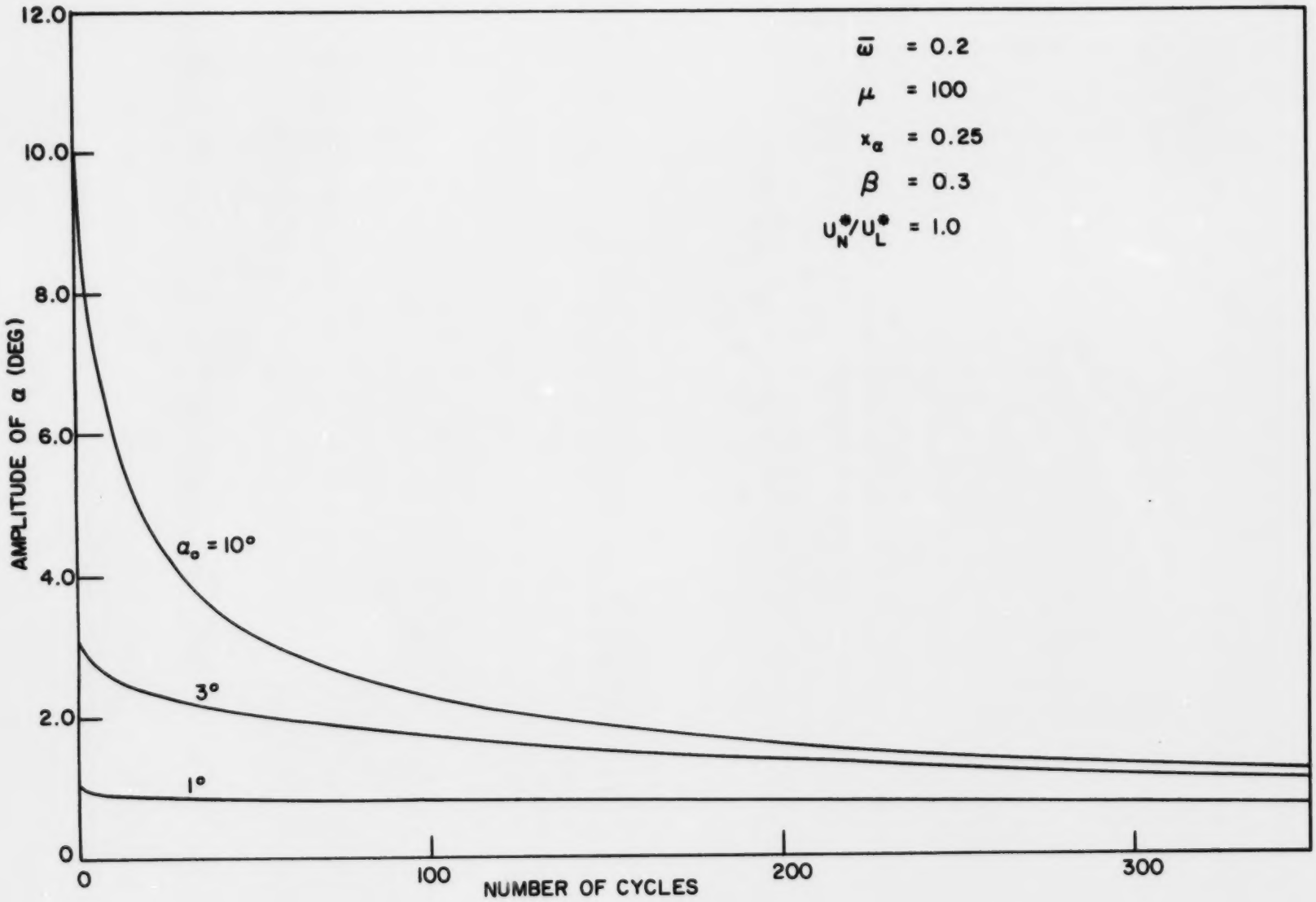

FIG. 9(b): VARIATION OF α WITH NUMBER OF CYCLES FOR $\bar{\omega}$ = 0.2, μ = 100, x_α = 0.25, β = 0.3 AND U_N^*/U_L^* = 1.0

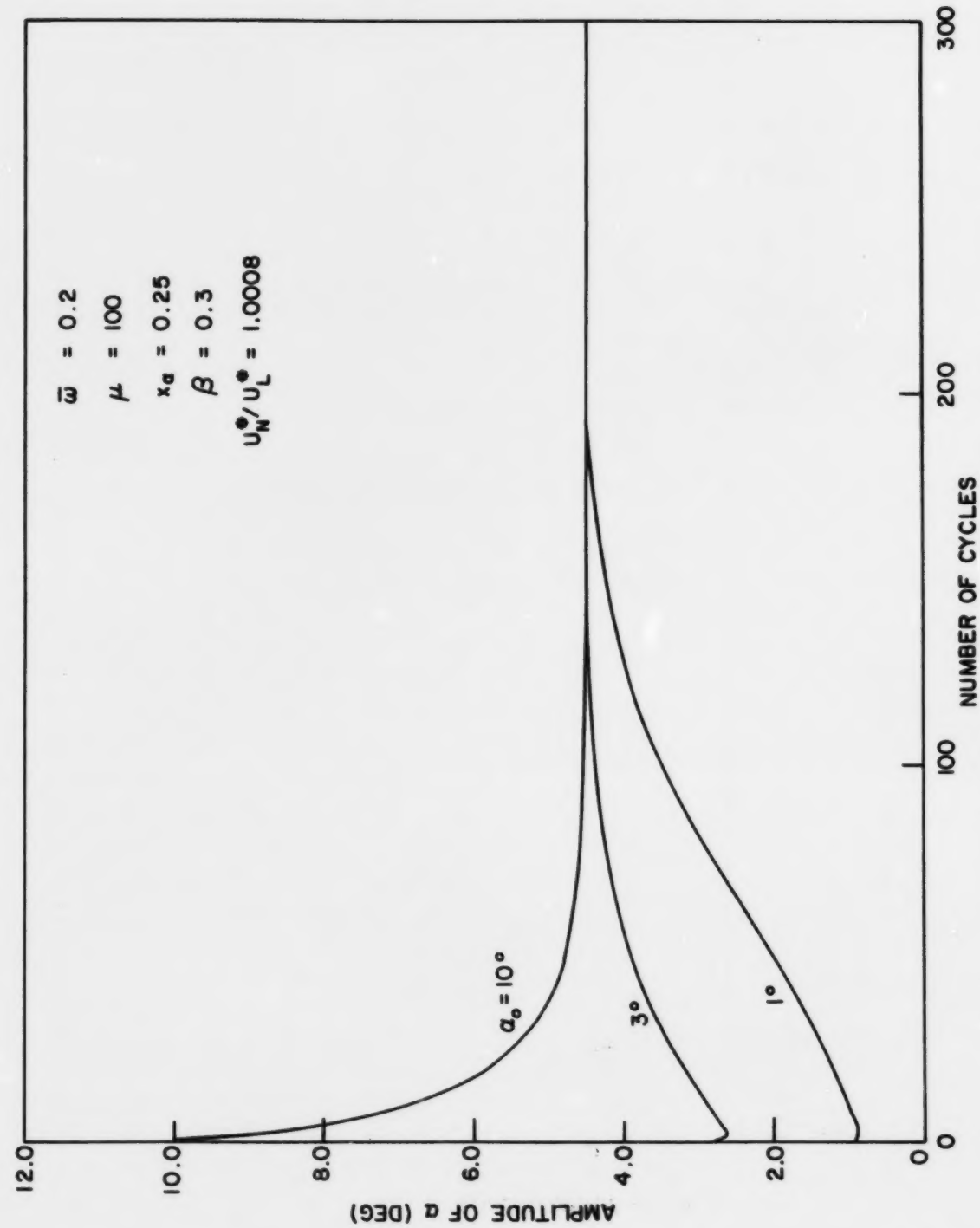

FIG. 9(c): VARIATION OF AMPLITUDE OF α WITH NUMBER OF CYCLES FOR $\bar{\omega}$ = 0.2, μ = 100, x_α = 0.25, β = 0.3 AND U_N^*/U_L^* = 1.0008

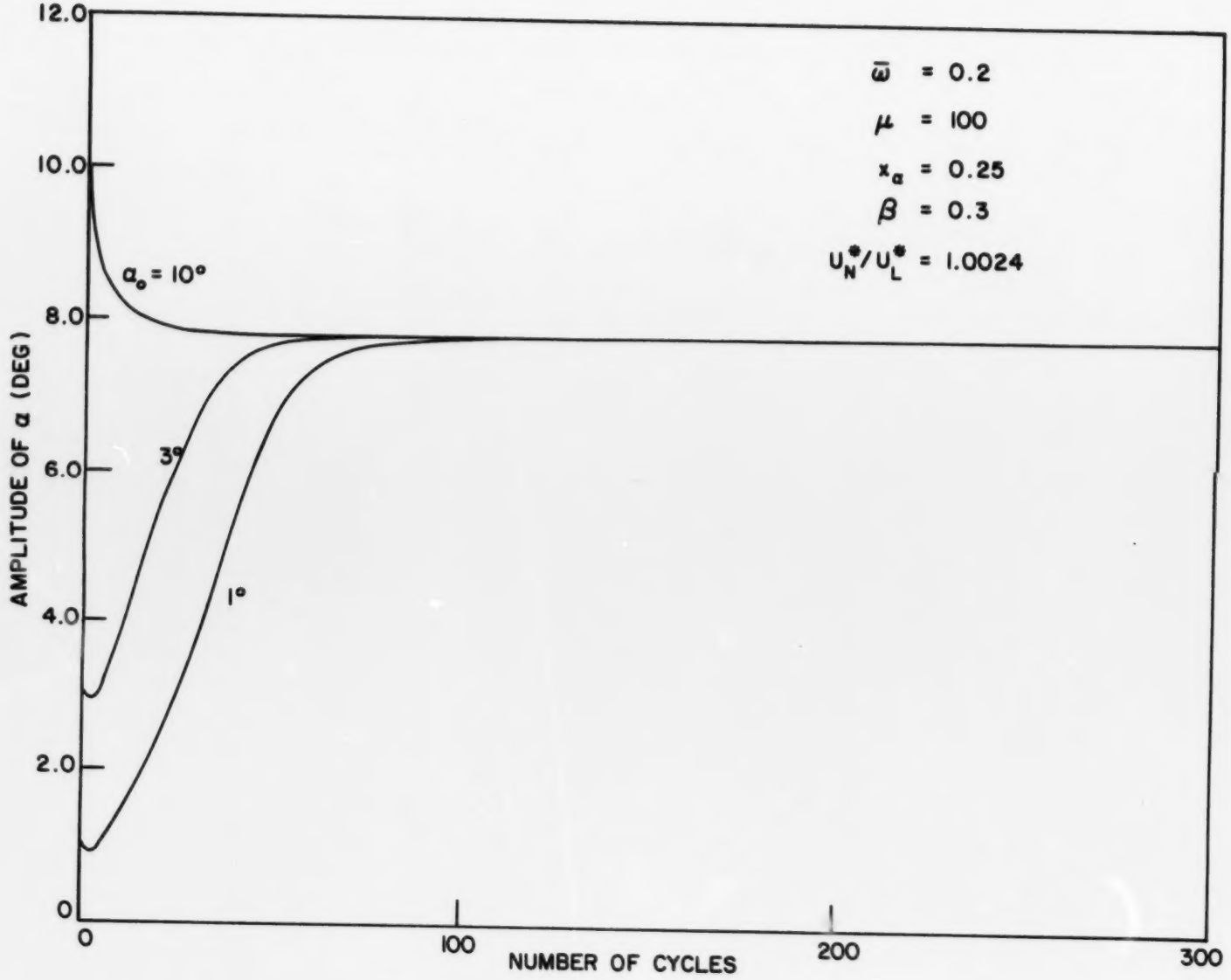

FIG. 9(d): VARIATION OF AMPLITUDE OF α WITH NUMBER OF CYCLES FOR $\bar{\omega}$ = 0.2, μ = 100, x_α = 0.25, β = 0.3 AND U_N^*/U_L^* = 1.0024

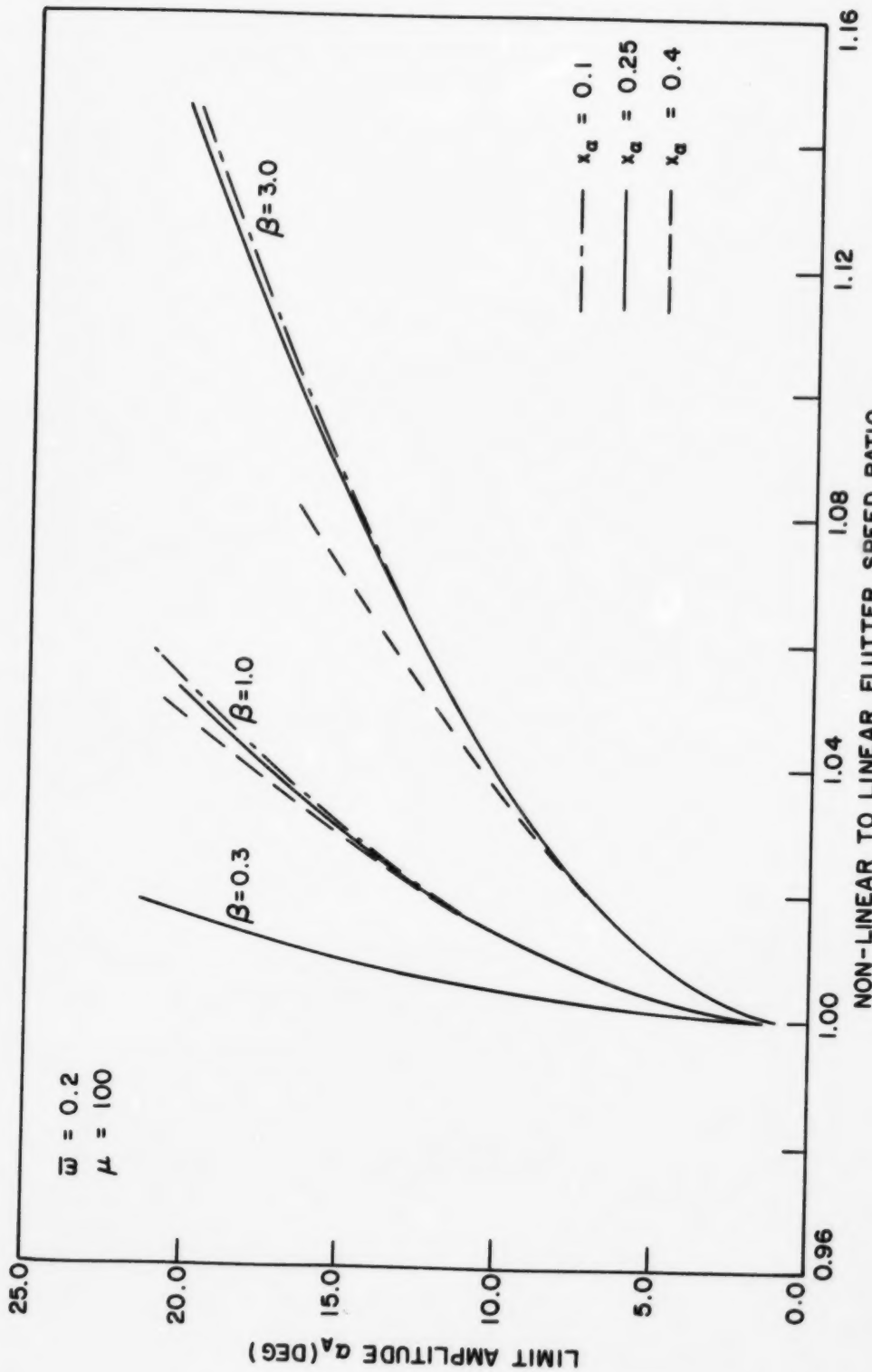

FIG. 10: VARIATION OF LIMIT-AMPLITUDE α_A WITH NON-LINEAR TO LINEAR FLUTTER SPEED RATIO FOR $\bar{\omega}$ = 0.2 AND μ = 100

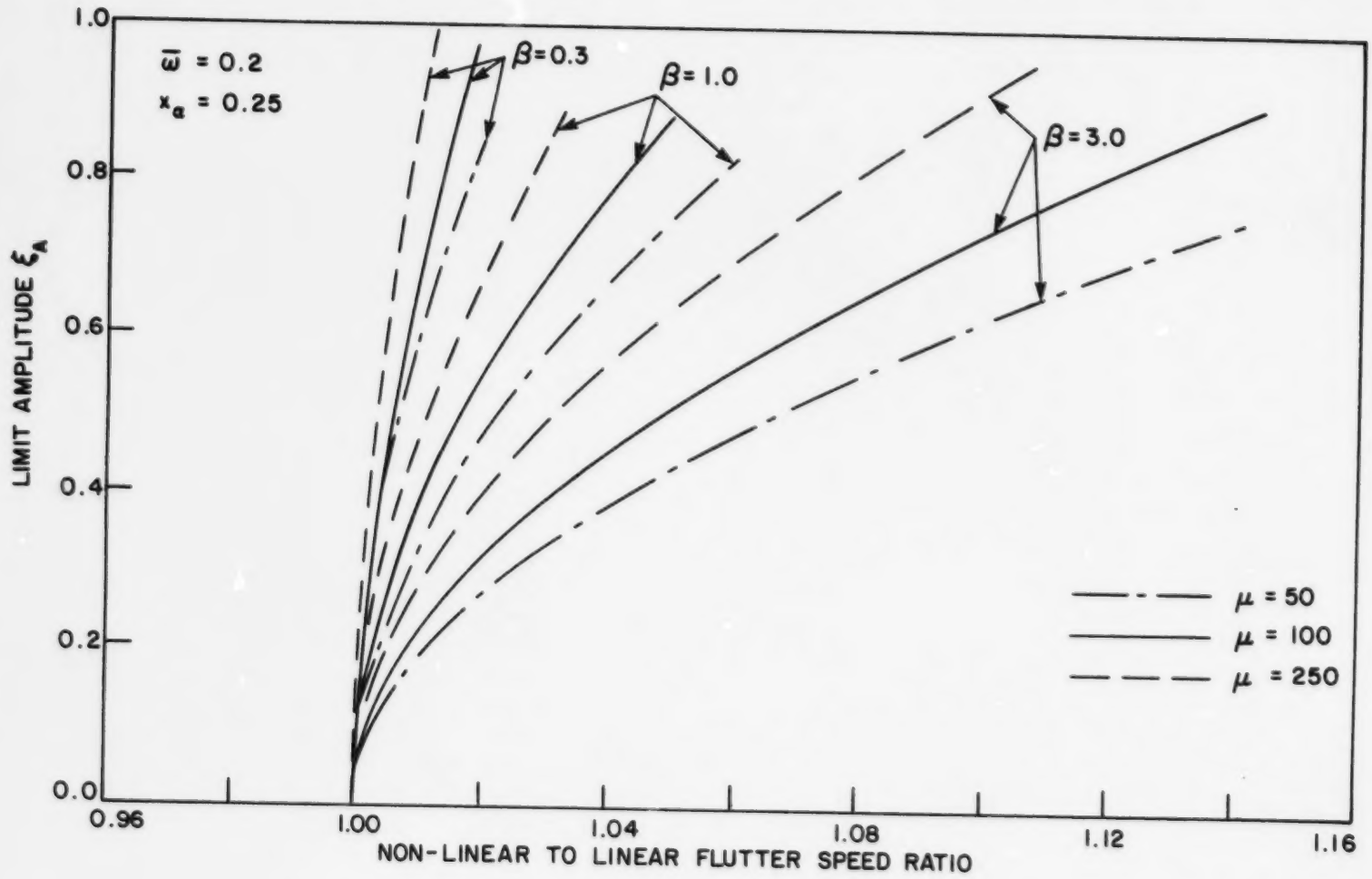

FIG. 11: VARIATION OF LIMIT-AMPLITUDE ξ_A WITH NON-LINEAR TO LINEAR FLUTTER SPEED RATIO FOR $\bar{\omega}$ = 0.2 AND x_α = 0.25

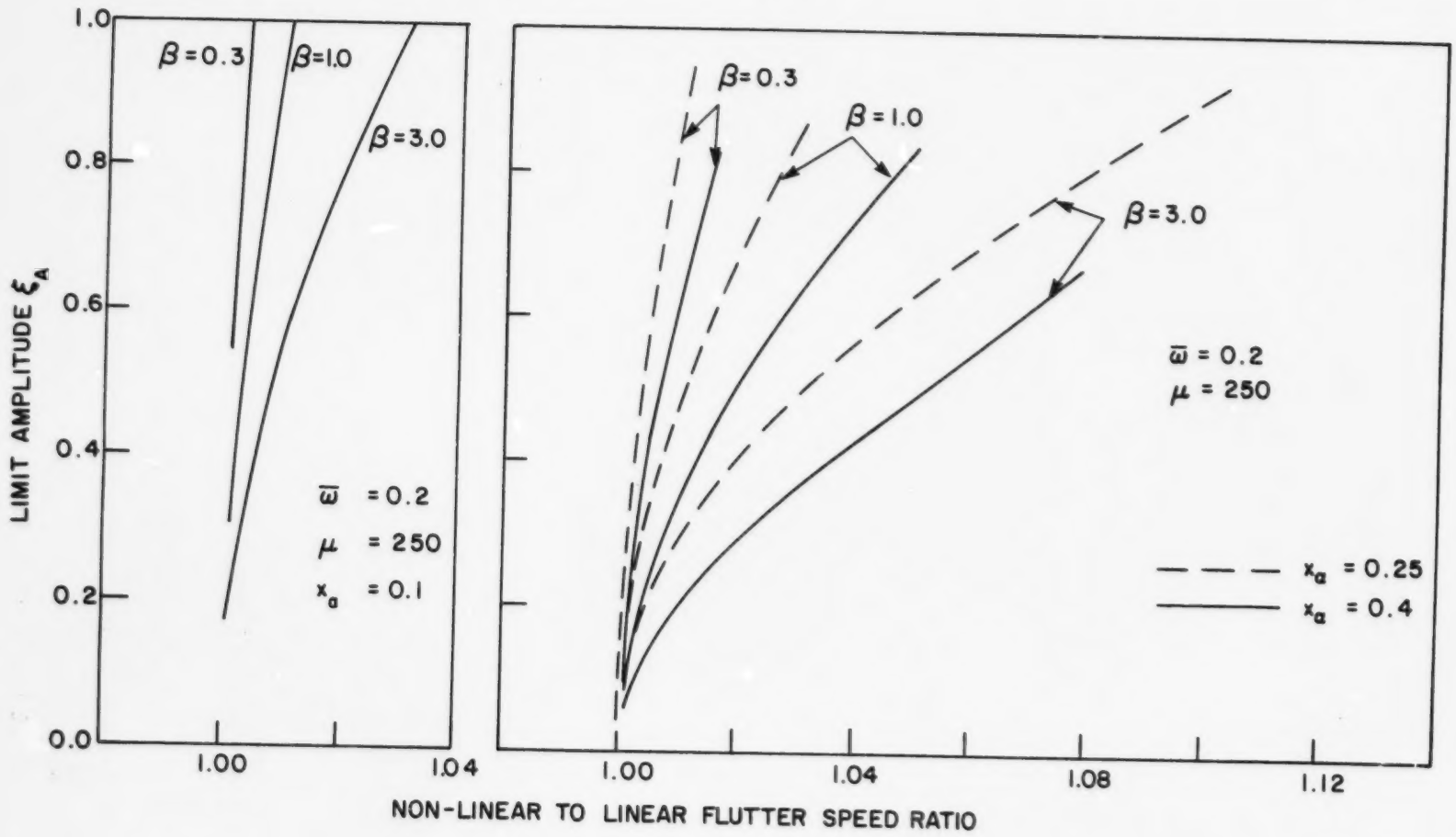

FIG. 12: VARIATION OF LIMIT-AMPLITUDE ξ_A WITH NON-LINEAR TO LINEAR FLUTTER SPEED RATIO FOR $\bar{\omega} = 0.2$ AND $\mu = 250$

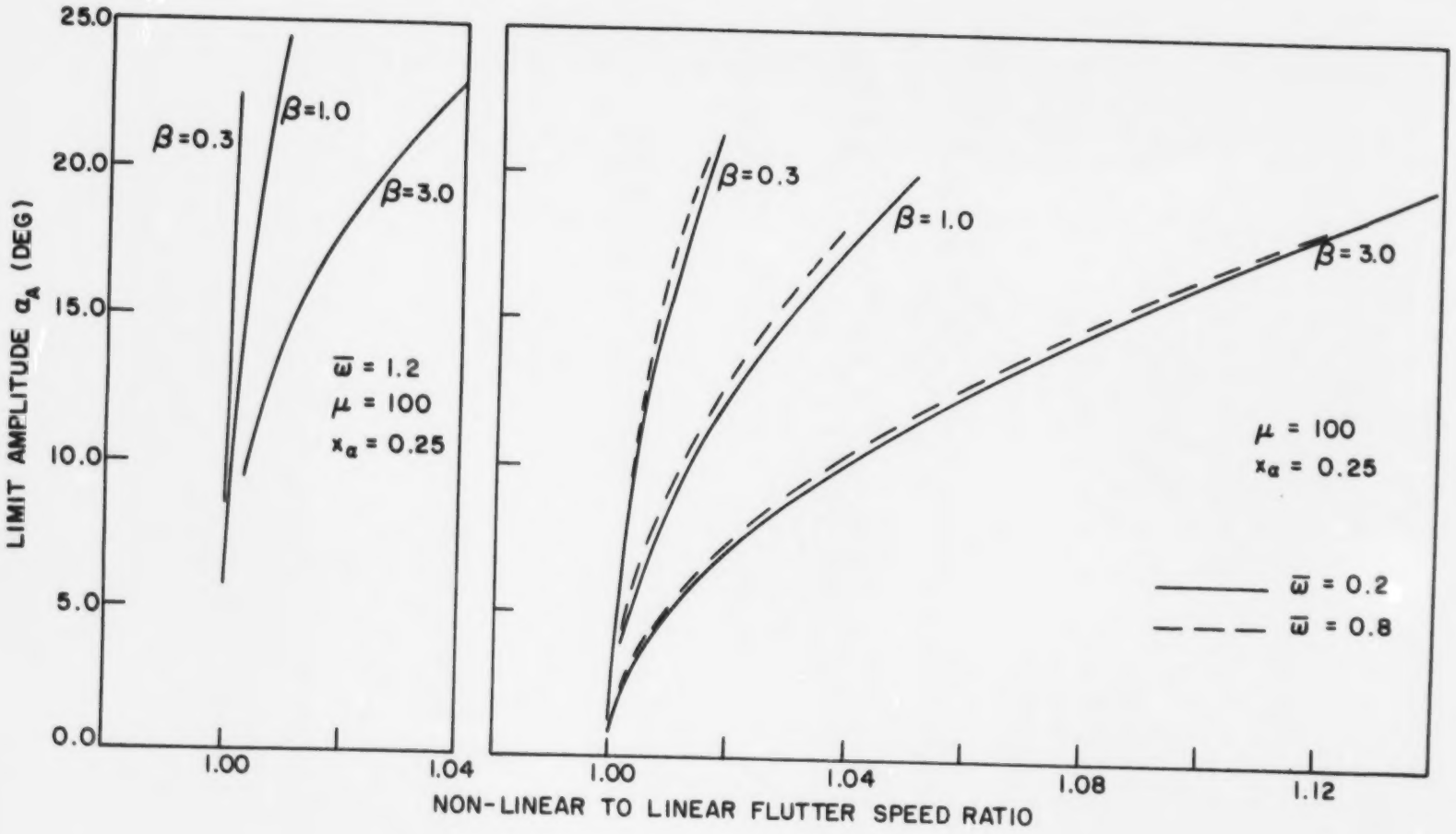

FIG. 13: VARIATION OF LIMIT-AMPLITUDE α_A WITH NON-LINEAR TO LINEAR FLUTTER SPEED RATIO FOR μ = 100 AND x_α = 0.25

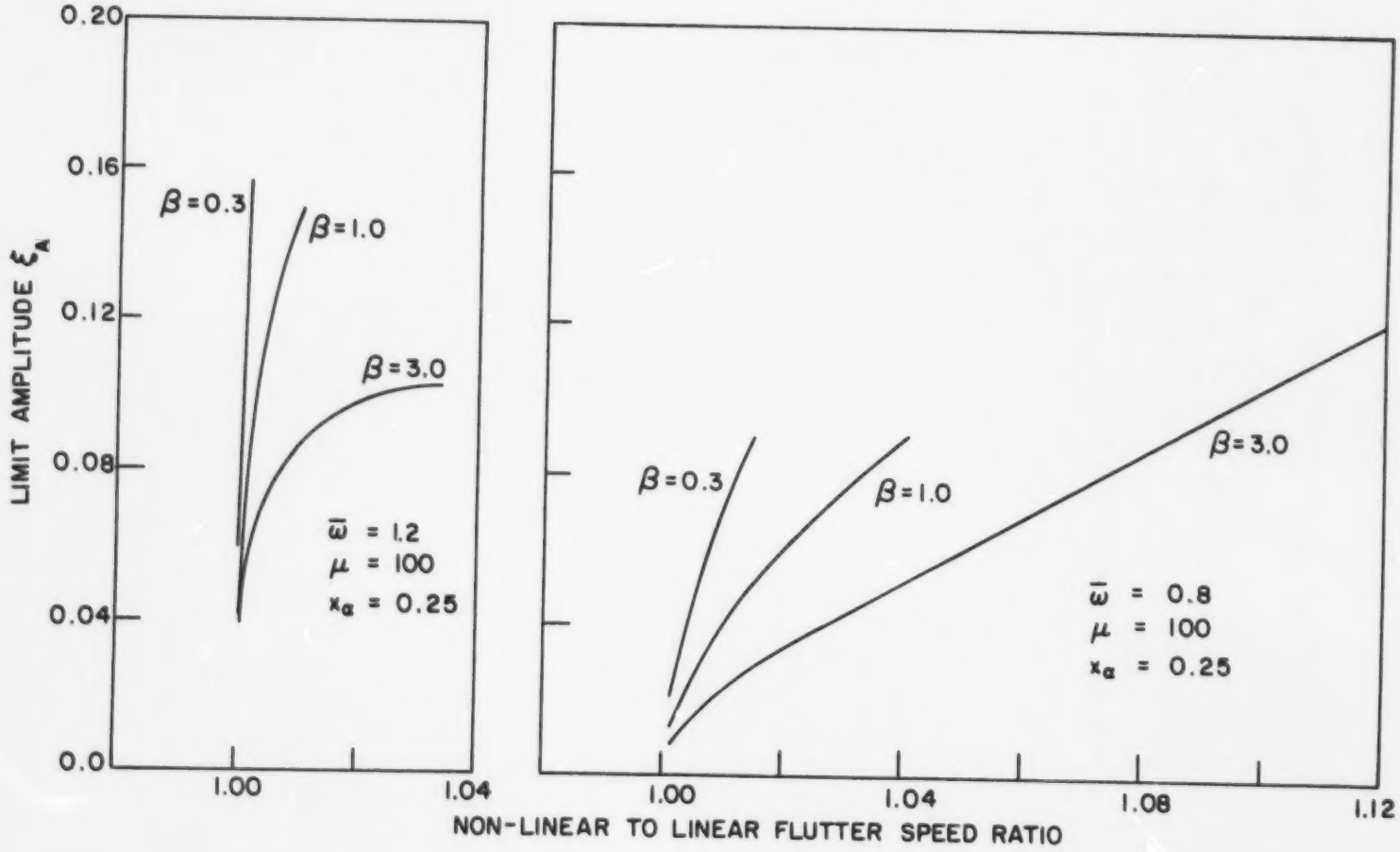

FIG. 14: VARIATION OF LIMIT-AMPLITUDE ξ_A WITH NON-LINEAR TO LINEAR FLUTTER SPEED RATIO FOR $\mu = 100$ AND $x_\alpha = 0.25$

APPENDIX A

The coefficients $\bar{E}$, $\bar{A}$, $\bar{I}$, $\bar{M}$ and the terms $\bar{U}$ and $\bar{T}$ on the RHS of Eqs. (13) and (14) are given as follows:

$$\bar{E} = E + \frac{1}{\mu r_\alpha^2 \Delta\tau^2} \tag{A1}$$

$$\bar{A} = A + \frac{2\bar{a}}{\mu r_\alpha^2} \tag{A2}$$

$$\bar{I} = I - V_1 \tag{A3}$$

$$\bar{M} = M - V_2 \tag{A4}$$

where

$$E = \frac{2x_\alpha}{r_\alpha^2 \Delta\tau^2}$$

$$A = \frac{2}{\Delta\tau^2} + \frac{11}{3\Delta\tau}\frac{\zeta_\alpha}{U^*} + \frac{1}{U^{*2}}$$

$$\bar{a} = \frac{3}{8\Delta\tau^2} + \frac{11}{12\Delta\tau}$$

$$I = \frac{2x_\alpha}{\Delta\tau^2}$$

$$V_1 = -\bar{e} - \frac{2}{\mu}\sigma_\alpha$$

$$M = \frac{2}{\Delta\tau^2} + \frac{11}{3\Delta\tau}\zeta_\xi\frac{\bar{\omega}}{U^*} + \frac{\bar{\omega}^2}{U^{*2}}$$

$$V_2 = -\frac{2}{\mu\Delta\tau^2} - \frac{2}{\mu}\sigma_\xi$$

and

$$\bar{e} = \frac{1}{\mu\Delta\tau^2} + \frac{11}{6\mu\Delta\tau}$$

$$\sigma_\alpha = \ell\left(1 + \frac{11}{6\Delta\tau}\right) - \frac{3}{8}\left(\frac{2}{\Delta\tau} + \frac{11}{6}\right)(a + c) \tag{A5}$$

$$\sigma_\xi = \frac{11\ell}{6\Delta\tau} - \frac{3}{4\Delta\tau}(a + c) \tag{A6}$$

ℓ, a and c are constants defined in Eq. (10). The RHS of Eq. (14) is given by

$$\bar{T} = \left(F + \frac{5}{2\mu r_\alpha^2 \Delta\tau^2}\right)\xi_\tau - \left(G + \frac{2}{\mu r_\alpha^2 \Delta\tau^2}\right)\xi_{\tau-\Delta\tau}$$

$$+ \left(H + \frac{1}{2\mu r_\alpha^2 \Delta\tau^2}\right)\xi_{\tau-2\Delta\tau} + \left(B + \frac{2\bar{b}}{\mu r_\alpha^2}\right)\alpha_\tau$$

$$- \left(C + \frac{2\bar{c}}{\mu r_\alpha^2}\right)\alpha_{\tau-\Delta\tau} + \left(D + \frac{2\bar{d}}{\mu r_\alpha^2}\right)\alpha_{\tau-2\Delta\tau}$$

$$+ \bar{Q}(\tau+\Delta\tau) \qquad \text{(A7)}$$

where

$$\bar{Q}(\tau+\Delta\tau) = \frac{Q(\tau+\Delta\tau)}{mU^2 r_\alpha^2}$$

is the non-dimensional external applied moment and

$$F = \frac{5x_\alpha}{r_\alpha^2 \Delta\tau^2}$$

$$G = \frac{4x_\alpha}{r_\alpha^2 \Delta\tau^2}$$

$$H = \frac{x_\alpha}{r_\alpha^2 \Delta\tau^2}$$

$$B = \frac{5}{\Delta\tau^2} + \frac{6\zeta_\alpha}{U^*\Delta\tau}$$

$$C = \frac{4}{\Delta\tau^2} + \frac{3\zeta_\alpha}{U^*\Delta\tau}$$

$$D = \frac{1}{\Delta\tau^2} + \frac{2\zeta_\alpha}{3U^*\Delta\tau}$$

$$\bar{b} = \frac{15}{16\Delta\tau^2} + \frac{3}{2\Delta\tau}$$

$$\bar{c} = \frac{3}{4\Delta\tau^2} + \frac{3}{4\Delta\tau}$$

$$\bar{d} = \frac{3}{16\Delta\tau^2} + \frac{1}{6\Delta\tau}$$

In deriving $\bar{U}$ of Eq. (13), Eq. (18) and (19) are used. The expressions for σ_α and σ_ξ have already been given in Eqs. (A5) and (A6), and λ_α and λ_ξ are given by the following:

$$\lambda_\alpha = p\ell + a\,K\,J_{1\alpha}(\tau) + c\,K\,J_{2\alpha}(\tau) - aq_1 - cq_2 \tag{A8}$$

$$\lambda_\xi = m\ell + a\,K\,J_{1\xi}(\tau) + c\,K\,J_{2\xi}(\tau) - an_1 - cn_2 \tag{A9}$$

where

$$p = \frac{1}{6\Delta\tau}\left(-18\alpha_\tau + 9\alpha_{\tau-\Delta\tau} - 2\alpha_{\tau-2\Delta\tau}\right) - \alpha'_\tau - \alpha_\tau$$

$$K = \frac{4x_\alpha}{\Delta\tau^2}$$

$$J_{1\alpha}(\tau) = e^{-b\tau}\int_0^\tau [\alpha''(\sigma) + \alpha'(\sigma)]e^{b\sigma}d\sigma$$

$$J_{2\alpha}(\tau) = e^{-d\tau}\int_0^\tau [\alpha''(\sigma) + \alpha'(\sigma)]e^{d\sigma}d\sigma$$

$$q_1 = \frac{3}{8}\left\{-\left(\frac{5}{\Delta\tau} + 3\right)\alpha_\tau + \left(\frac{4}{\Delta\tau} + \frac{3}{2}\right)\alpha_{\tau-\Delta\tau} - \left(\frac{1}{\Delta\tau} + \frac{1}{3}\right)\alpha_{\tau-2\Delta\tau}\right\}$$
$$+ \frac{\Delta\tau}{24}\left\{19e^{-b\Delta\tau}\left(\alpha''_\tau + \alpha'_\tau\right) - 5e^{-2b\Delta\tau}\left(\alpha''_{\tau-\Delta\tau} + \alpha'_{\tau\Delta\tau}\right)\right.$$
$$\left. + e^{-3b\Delta\tau}\left(\alpha''_{\tau-2\Delta\tau} + \alpha'_{\tau-2\Delta\tau}\right)\right\}$$

$$q_2 = \frac{3}{8}\left\{-\left(\frac{5}{\Delta\tau} + 3\right)\alpha_\tau + \left(\frac{4}{\Delta\tau} + \frac{3}{2}\right)\alpha_{\tau-\Delta\tau} - \left(\frac{1}{\Delta\tau} + \frac{1}{3}\right)\alpha_{\tau-2\Delta\tau}\right\}$$
$$+ \frac{\Delta\tau}{24}\left\{19e^{-d\Delta\tau}\left(\alpha''_\tau + \alpha'_\tau\right) - 5e^{-2d\Delta\tau}\left(\alpha''_{\tau-\Delta\tau} + \alpha'_{\tau-\Delta\tau}\right)\right.$$
$$\left. + e^{-3d\Delta\tau}\left(\alpha''_{\tau-2\Delta\tau} + \alpha'_{\tau-2\Delta\tau}\right)\right\}$$

$$m = \frac{1}{6\Delta\tau}\left(-18\,\xi_\tau + 9\xi_{\tau-\Delta\tau} - 2\xi_{\tau-2\Delta\tau}\right) - \xi'_\tau$$

$$J_{1\xi}(\tau) = e^{-b\tau}\int_0^\tau \xi''(\sigma)e^{b\sigma}d\sigma$$

$$J_{2\xi}(\tau) = e^{-d\tau}\int_0^\tau \xi''(\sigma)e^{d\sigma}d\sigma$$

$$n_1 = \frac{3}{8\Delta\tau}\left(-5\xi_\tau + 4\xi_{\tau-\Delta\tau} - \xi_{\tau-2\Delta\tau}\right)$$
$$- \frac{\Delta\tau}{24}\left(19e^{-b\Delta\tau}\,\xi''_\tau - 5e^{-2b\Delta\tau}\,\xi''_{\tau-\Delta\tau} + e^{-3b\Delta\tau}\,\xi''_{\tau-2\Delta\tau}\right)$$

$$n_2 = \frac{3}{8\Delta\tau}\left(-5\xi_\tau + 4\xi_{\tau-\Delta\tau} - \xi_{\tau-2\Delta\tau}\right)$$
$$+ \frac{\Delta\tau}{24}\left(19e^{-d\Delta\tau}\,\xi''_\tau - 5e^{-2d\Delta\tau}\,\xi''_{\tau-\Delta\tau} + e^{-3d\Delta\tau}\,\xi''_{\tau-2\Delta\tau}\right)$$

$\bar{U}$ can be written as follows:

$$\bar{U} = \bar{f}\alpha_\tau - \bar{g}\alpha_{\tau-\Delta\tau} + \bar{h}\alpha_{\tau-2\Delta\tau} + \frac{5}{\mu\Delta\tau^2}\,\xi_\tau$$
$$- \frac{4}{\mu\Delta\tau}\,\xi_{\tau-\Delta\tau} + \frac{1}{\mu\Delta\tau^2}\,\xi_{\tau-2\Delta\tau}$$
$$- \frac{2}{\mu}\,\phi(\tau+\Delta\tau)\,\left[\alpha(0) + \xi'(0) + \alpha'(0)\right] - \frac{2}{\mu}\left[I_\alpha(\tau) + I_\xi(\tau) + \lambda_\alpha + \lambda_\xi\right]$$
$$+ N\xi_\tau - P\xi_{\tau-\Delta\tau} + S\xi_{\tau-2\Delta\tau} + J\alpha_\tau - K\alpha_{\tau-\Delta\tau}$$
$$+ L\alpha_{\tau-2\Delta\tau} + \bar{P}(\tau+\Delta\tau) \qquad \text{(A10)}$$

and

$$\bar{f} = \frac{5}{2\mu\Delta\tau^2} + \frac{3}{\mu\Delta\tau}$$

$$\bar{g} = \frac{2}{\mu\Delta\tau^2} + \frac{3}{2\mu\Delta\tau}$$

$$\bar{h} = \frac{1}{2\mu\Delta\tau^2} + \frac{1}{3\mu\Delta\tau}$$

$$N = \frac{5}{\Delta\tau^2} + 6\,\frac{\zeta_\xi}{\Delta\tau}\,\frac{\bar{\omega}}{U^*}$$

$$P = \frac{4}{\Delta\tau^2} + 3\,\frac{\zeta_\xi}{\Delta\tau}\,\frac{\bar{\omega}}{U^*}$$

$$S = \frac{1}{\Delta\tau^2} + \frac{2}{3}\,\frac{\zeta_\xi}{\Delta\tau}\,\frac{\bar{\omega}}{U^*}$$

$$J = \frac{5x_\alpha}{\Delta\tau^2}$$

$$L = \frac{x_\alpha}{\Delta\tau^2}$$

$\bar{P}(\tau+\Delta\tau)$ is the non-dimensional external applied force given by

$$\bar{P}(\tau+\Delta\tau) = \frac{bP(\tau+\Delta\tau)}{mU^2}$$

APPENDIX B

The terms ψ_1^n and ψ_2^n with n = 2, 3 and 4 in Eqs. (26) and (27) are given as follows:

$$\psi_1^2 = -2\zeta_\xi \frac{\bar{\omega}}{U^*} \xi_o' - \left(\frac{\bar{\omega}}{U^*}\right)^2 (\xi_o + \theta\xi_o^3) - \frac{\alpha_o'}{\mu} - \frac{2}{\mu} \phi(0)\, w(0) + \bar{P}_o \tag{B1}$$

$$\psi_2^2 = -\left(\frac{2\zeta_\alpha}{U^*} + \frac{1}{\mu r_\alpha^2}\right)\alpha_o' - \frac{1}{U^{*2}} (\alpha_o + \beta\, \alpha_o^3) + \bar{Q}_o \tag{B2}$$

$$\psi_1^3 = -2\zeta_\xi \frac{\bar{\omega}}{U^*} \xi_o'' - \left(\frac{\bar{\omega}}{U^*}\right)^2 (1 + 3\theta\, \xi_o^2)\xi_o' - \frac{1}{\mu} \alpha_o'' - \frac{2}{\mu} w(0)\phi'(0) - \frac{2}{\mu} \phi(0)\, (\xi_o'' + \alpha_o'' + \alpha_o') + \bar{P}_o' \tag{B3}$$

$$\psi_2^3 = -\left(\frac{2\zeta_\alpha}{U^*} + \frac{1}{\mu r_\alpha^2}\right)\alpha_o'' - \frac{\alpha_o'}{U^{*2}} (1 + 3\beta\alpha_o^2) + \bar{Q}_o' \tag{B4}$$

$$\psi_1^4 = -2\zeta_\xi \frac{\bar{\omega}}{U^*} \xi_o''' - \left(\frac{\bar{\omega}}{U^*}\right)^2 \{(1 + 3\theta\xi_o^2)\xi_o'' + 6\theta\xi_o \xi_o'^2\} - \frac{1}{\mu} \alpha_o''' - \frac{2}{\mu} w(0)\phi''(0) - \frac{2}{\mu} \{\phi(0)(\xi_o''' + \alpha_o''' + \alpha_o'') + (ab + cd)\, (\xi_o'' + \alpha_o'' + \alpha_o')\} + \bar{P}_o'' \tag{B5}$$

$$\psi_2^4 = -\left(\frac{2\zeta_\alpha}{U^*} + \frac{1}{\mu r_\alpha^2}\right)\alpha_o''' - \frac{1}{U^{*2}} \{(1 + 3\beta\alpha_o^2)\, \alpha_o'' + 6\beta\, \alpha_o\, \alpha_o'^2\} + \bar{Q}_o'' \tag{B6}$$

where

$$w(0) = \alpha(0) + \xi'(0) + \alpha'(0)$$

$$\phi(0) = \ell - a - c$$

$$\phi'(0) = ab + cd$$

$$\phi''(0) = -(ab^2 + cd^2)$$

REPORT DOCUMENTATION PAGE / PAGE DE DOCUMENTATION DE RAPPORT

REPORT/RAPPORT 1a	REPORT/RAPPORT 1b
NAE-AN-36	NRC No. 25438
REPORT SECURITY CLASSIFICATION / CLASSIFICATION DE SÉCURITÉ DE RAPPORT 2	DISTRIBUTION (LIMITATIONS) 3
Unclassified	Unlimited

TITLE/SUBTITLE/TITRE/SOUS-TITRE 4

Flutter Analysis of a Two-Dimensional Airfoil with Cubic Non-Linear Restoring Force

AUTHOR(S)/AUTEUR(S) 5

B.H.K. Lee, P. LeBlanc

SERIES/SÉRIE 6

Aeronautical Note

CORPORATE AUTHOR/PERFORMING AGENCY/AUTEUR D'ENTREPRISE/AGENCE D'EXÉCUTION 7

National Research Council Canada
National Aeronautical Establishment — High Speed Aerodynamics Laboratory

SPONSORING AGENCY/AGENCE DE SUBVENTION 8

DATE 9	FILE/DOSSIER 10	LAB. ORDER / COMMANDE DU LAB. 11	PAGES 12a	FIGS/DIAGRAMMES 12b
86-02			47	14

NOTES 13

DESCRIPTORS (KEY WORDS)/MOTS-CLÉS 14

1. Flutter — analysis
2. Aerofoils — flutter

SUMMARY/SOMMAIRE 15

Flutter analysis of a two-dimensional airfoil with a cubic non-linear restoring force in the pitch degree of freedom is investigated. The structural dynamic equations of motion are integrated by a time marching finite difference scheme. Flutter is determined from conditions which give rise to either a divergent or limit-amplitude solution. Case studies using various airfoil parameters and coefficients of the non-linear term in the restoring force are carried out. The effect of initial conditions is studied by varying the displacement from equilibrium of the pitch angle at the start of the airfoil motion. For a soft spring, an increase in the initial angular displacement can induce flutter to occur below the linear flutter speed. Factors that have stabilizing and destabilizing effects are investigated. For a hard spring, divergent flutter is not encountered. Instead, the oscillations maintain a self-limited amplitude which is independent of initial angular displacement. The effects of airfoil parameters on the amplitudes of heave and pitch motions are studied.